

## A Closer Look at Mortality Risk Prediction from Electrocardiograms

Platon Lukyanenko, PhD<sup>a,c</sup>, Joshua Mayourian, MD<sup>b,c</sup>, Mingxuan Liu, MS<sup>a,d</sup>,  
John K. Triedman, MD<sup>b,c</sup>, Sunil J. Ghelani, MD<sup>b,c</sup>, William G. La Cava, PhD<sup>a,c,\*</sup>

<sup>a</sup>Computational Health Informatics Program, Boston Children's Hospital

<sup>b</sup>Department of Cardiology, Boston Children's Hospital

<sup>c</sup>Department of Pediatrics, Harvard Medical School

<sup>d</sup>National University of Singapore

\*Correspondence: [william.lacava@childrens.harvard.edu](mailto:william.lacava@childrens.harvard.edu). 617-355-6000

Lab page: <https://cavalab.org>

## Abstract

**Background.** Several recent studies combine large private electrocardiographic (ECG) databases with artificial intelligence (AI-ECG) to predict patient mortality. These studies typically use a few, highly variable, modeling approaches. While benchmarking these approaches has historically been limited by a lack of public ECG datasets, this changed with the 2023 release of MIMIC-IV, containing 795,546 ECGs from a U.S. hospital system, and the 2020 release of Code-15, containing 345,779 ECGs collected during routine care in Brazil.

**Methods.** We benchmark over 500 AI-ECG survival models predicting all-cause mortality on Code-15 and MIMIC-IV with two neural architectures, four Deep-Survival-Analysis approaches, and classifiers predicting mortality at four time horizons, along with several simpler baselines. We extend the highest-performing approach to a dataset from Boston Children's Hospital (BCH, 225,379 ECGs) that is predominantly sourced from a pediatric and congenital heart disease cohort. Models train with and without demographics (age/sex) and evaluate across datasets.

**Findings.** The best performing Deep-Survival-Analysis models trained with ECG and demographics yield good median Concordance Indices (Code-15: 0.82, MIMIC-IV: 0.78, BCH: 0.76) and AUPRC scores (median 1-yr/5-yr, Code-15: 0.07/0.15; MIMIC-IV: 0.45/0.55; BCH: 0.04/0.13) considering the percentage of ECGs linked to mortality (1-yr/5-yr, Code-15: 1.2%/3.4%; MIMIC-IV: 14.8%/24.5%; BCH: 0.9%/4.8%). Contrasting with Deep-Survival-Analysis models, classifier-based AI-ECG models exhibit significant, site-dependent sensitivity to the choice of time horizon (median Pearson's  $R$ , Code-15: 0.69,  $p < 1E-5$ ; MIMIC-IV: -0.80  $p < 1E-5$ ). Some demographic-only models perform surprisingly well compared to ECG-only models (Code-15: median concordance 0.79). Model concordance drops 0.03-0.24 on external validation.

**Interpretation.** We recommend Deep-Survival-Analysis over Classifier-Cox approaches and the inclusion of demographic covariates in ECG survival modeling. Comparisons to simpler demographic-only and baseline models is crucial. External evaluations highlight how care setting (e.g., acuity) affects model transferability and support fine-tuning models on site-specific data.

**Funding.** Thrasher Research Fund. Boston Children's Hospital. NIH. NLM. NICDHD. Kosten Innovation Fund.

## Research In Context

### Evidence before this study

Several recent studies apply artificial intelligence to electrocardiography (AIECG) to predict patient mortality. These studies typically train AIECG models on private datasets and report results for a single approach involving one ECG interpretation method and one survival analysis method (e.g. a convolutional neural network classifier predicting five-year mortality followed by a Cox regression).

Among PubMed publications 2019-2024 (*Criteria: (Mortality[Title] OR Death[Title]) AND (prediction OR risk) AND (ECG OR electrocardiography OR electrocardiogram) AND (machine learning OR deep learning)*), 14 of 40 studies trained AIECG on more than 25,000 ECGs. These 14 studies trained on private datasets, employed at least 12 different ECG interpretation methods, and fewer than half explicitly compare their models to simpler baselines. This fractured approach obscures AIECG impact and limits the development of verifiable best practices and publicly available models.

### Added value of this study

We build and evaluate over five hundred all-cause mortality prediction models. We benchmark two recently released public datasets using two ECG interpretation architectures, eight survival analysis methods (four Deep-Survival-Analysis methods and Cox regressions following classifiers predicting mortality at four different time horizons), along with simpler baselines. We then use the top performing approach to model all-cause mortality in a primarily congenital-heart-defect pediatric dataset. All code is released publicly.

### Implications of all the available evidence

We recommend using Deep-Survival-Analysis and including demographic covariates in ECG survival modeling. Comparisons to simple baseline models (e.g. demographic-only models) are crucial to establishing the added value of AIECG. Training data setting (e.g., acuity) affects model transferability, encouraging model fine-tuning on site-specific data.

# Background

Electrocardiography (ECG) measures the electric activity of the heart, and abnormal 12-channel ECGs often indicate cardiovascular pathology and are thus a marker for disease and mortality. AI-ECG refers to the application of AI or machine learning to ECG[1]. A common AI-ECG task is risk stratification, which is equivalent to predicting event occurrence (e.g. mortality or passing a diagnostic threshold). Several studies have recently applied AI-ECG to predict patient outcomes including mortality risk[1–5], ventricular hypertrophy[6], and ventricular dysfunction in both adults[7] and children[8]. While these studies demonstrate AI-ECG’s potential value, most use private data and provide results for only several modeling approaches. Consequently, there is no consensus on preferred modeling approach (e.g. deep learning or survival modeling algorithms).

Most studies train AI-ECG models on large private ECG datasets (ex, ECGs: 2·4M[9], 2·3M[4]; 1·2M[10]) or fine-tune accessible models[1,11,12]. However, verifiably evaluating different modeling approaches and creating verifiable public ECG models requires large, public ECG datasets linked to high-quality patient-level data. Fortunately, such data has recently become more available with the public releases of the MIMIC-IV dataset (800k ECGs) in 2023[13-14] and the Code-15 dataset (345k ECGs) in 2020[15]. See[16] for a list of public datasets pre-2020.

Given these new datasets and the high interest in risk prediction from ECGs, a benchmark establishing the performance of common deep learning architectures and survival modeling approaches could inform future AI-ECG studies. We create and analyze such a benchmark here, modeling all-cause patient mortality from ECG across two architectures and eight survival modeling configurations on MIMIC-IV and Code-15. We then use the best-performing approach to model all-cause mortality on a private dataset from Boston Children's Hospital (BCH).

# Methods

## Overview

We first benchmark survival analysis approaches on two public ECG datasets (Code-15 and MIMIC-IV), and then use the best performing approach to model survival in a third, private, ECG dataset (BCH). The dataset cohorts are described in **(Table 1)**. We then evaluate the best performing approach within and across sites, comparing it to baselines 1) trained only on demographics and/or 2) trained using gradient boosting with extracted ECG features. Lastly, we explore the impacts of model architecture, survival modeling approach, and inclusion of demographic data, across sites, classifier time horizons, and patient subgroups.

## Datasets

Table 1

	Measure	Unit	All	Event	Non-Event	P value
	<b>Code-15</b>	ECGs	N (%)	233,647	8,341 (3.6%)	225,306 (96.4%)
Patients		N (%)	233,647	8,341 (3.6%)	225,306 (96.4%)	
Female		N (%)	138,911 (59.4%)	3,853 (2.8%)	135,058 (97.2%)	<< 1E-5
Male		N (%)	947,36 (40.6%)	4,488 (4.7%)	90,248 (95.3%)	
Age		Yr (Std)	50.7 (19.8)	70.4 (14.0)	50.0 (19.6)	<< 1E-5
Followup	Yr (Std)	3.7 (1.9)	2.0 (1.6)	3.7 (1.8)	<< 1E-5	
	Measure	Unit	All	Event	Non-Event	P value
	<b>MIMIC-IV</b>	ECGs	N (%)	785,035	215,039 (27.4%)	569,996 (72.6%)
Patients		N (%)	159,122	25,107 (15.8%)	134,015 (84.2%)	
Female		N (%)	384,923 (49.0%)	99,170 (25.8%)	285,753 (74.2%)	<< 1E-5
Male		N (%)	400,112 (51.0%)	115,869 (29.0%)	284,243 (71.0%)	
Age		Yr (Std)	64.23 (17.1)	72.52 (14.1)	61.14 (17.1)	<< 1E-5
Followup	Yr (Std)	2.7 (2.8)	2.0 (2.4)	3.0 (2.8)	<< 1E-5	
	Measure	Unit	All	Event	Non-Event	P value
	<b>BCH</b>	ECGs	N (%)	181,976	12,638 (6.9%)	169,338 (93.1%)
Patients		N (%)	50,447	16,71 (3.3%)	48,776 (96.7%)	
Female		N (%)	86,141 (47.3%)	6,048 (7.0%)	80,093 (93.0%)	0.23
Male		N (%)	95,835 (52.7%)	6,590 (6.9%)	89,245 (93.1%)	
Age		Yr Mean(Std)	12.8 (11.9)	21.5 (16.7)	12.2 (11.2)	<< 1E-5
Followup	Yr Mean(Std)	8.9 (6.7)	7.2 (6.1)	9.0 (6.7)	<< 1E-5	

Table 1. Population characteristics after data filtering. Note large differences in event rates and ages. Categorical comparisons: Chi-Square test; numerical: Student's T.

## Code-15

Code-15[15] is an ECG dataset from the Telehealth Network of Minas Gerais, a Brazilian public agency providing telehealth services to Minas Gerais and Amazonian and Northeast states. Patient

ECGs were recorded in primary care facilities by technicians and examined remotely by a cardiologist. The publicly available dataset includes 345,779 ECGs collected from April to September of 2018. Code15 ECGs are 7-10 second signals sampled at 400Hz, centered and padded with zeros to total a length of 4096.

The Code-15 Dataset provides multiple ECGs per subject and indicates the patient's age and the follow-up time after the patient's final ECG. We only use the one entry per subject that provides a specific follow-up time. Overall, we kept 233,647 ECGs; 1·23% / 2·07% / 3·36% / 3·61% of ECGs link to a mortality by year 1 / 2 / 5 / 7·67 (max).

## MIMIC-IV

The MIMIC-IV[13] dataset includes 795,546 ECGs from 159,608 patients collected between 2008-2019 at the Beth Israel Deaconess Medical Center in Boston, Massachusetts. Patient ECGs were recorded in various settings, including emergency settings, hospitals, and outpatient care centers. MIMIC-IV ECGs are 10 second signals sampled at 500Hz.

MIMIC-IV tracks date-of-death with state and hospital records, and censors deaths one year after a final recorded hospital visit. Overall, we kept 785,035 ECGs; 14·8% / 18·4% / 24·5% / 27·6% / 27·8% of ECGs link to a mortality by year 1 / 2 / 5 / 10 / 12·97(max).

For MIMIC-IV, we also explore models trained additionally with these automatic ECG measures: Axes – P, QRS, T; Durations – P, PQ, QRS, QT, RR. We do not adjust incorrect measures – such adjustments did not improve performance in early experiments.

## Boston Children's Hospital

The BCH[17] dataset includes 225,379 ECGs from 79,568 patients collected 1990 to 2018 at Boston Children's Hospital in Boston, Massachusetts from emergency, hospital, and outpatient care settings. This dataset predominantly represents a pediatric congenital heart disease cohort and differs drastically from adult cohorts due to structural and age-dependent causes. BCH ECGs were resampled to the Code-15 standard. Death was tracked by an internal institutional database. Overall, we kept 181,976 ECGs; 0·9% / 1·5% / 3·1% / 4·8% / 6·9% are associated with a mortality by year 1/2/5/10/33(max).

## Dataset processing

Dataset preparation is illustrated in **Figure 1**. Data is limited to [Patient ID, Time-To-Event, Event, ECG, Age, Sex, Machine Measures (MIMIC-IV only)], and entries with missing ECG samples or Time-To-Event are excluded. Time-To-Event is set to a minimum of 0·5 days. MIMIC-IV and BCH ECGs are re-sampled to 10 seconds at 400Hz and padded with 48 starting/trailing zeros for an end shape of 4096 x 12. Code-15 and MIMIC data is split 64/16/20 into train/validation/test sets randomly by patient ID. BCH data is split 42/8/50 into train/validation/test by patient ID[17]. The random seed sets the Training/Validation split while the Test set remains fixed. Before model training or evaluation, all ECGs were z-score normalized per ECG channel based on the model's training set.

## Survival analysis

Survival analysis builds survival functions,  $S(t)$ , that denote the probability of not having experienced an Event by a time  $t$ . Survival analysis uses data in the form [Time-To-Event, Event], which denotes Event state at a follow-up time. This leverages information even when final event time is unknown: a device that works for two years before being lost still provides two years of evidence of non-breakage. ‘Censoring’ refers to not knowing event outcomes for some subjects.

The most common survival functions are Kaplan-Meier curves which display survival over time from a tracked population. If the population is clustered into groups, an individual’s trajectory can be estimated from their cluster’s survival function. Otherwise, survival functions usually fit an exponential decay or Weibull function to regressors (demographics, measurements, etc.).

The Cox proportional hazards model[18] models hazard,  $h(t) = d/dt (1 - S(t))$ , as an unknown base function scaled by exponential decays:  $h(t) = h_0(t)\exp(\beta_1x_1 + \beta_2x_2 + \dots + \beta_mx_m)$  where  $\{x_1, \dots, x_m\}$  are regressors and  $\{\beta_1, \dots, \beta_m\}$  are learned weights. The Breslow estimator is often used to fit  $h_0(t)$ [19]. The Cox regression assumes that *log-risk* ( $\beta_1x_1 + \beta_2x_2 + \dots + \beta_mx_m$ ) is *proportional* (e.g. smoker risk / non-smoker risk = constant) and a *linear* function of regressors that is *time-constant* (there are no time-regressor interactions).

There are two broad approaches to survival modeling with neural networks:

*Classifier-Cox*: The first approach interprets inputs into a set of values with a neural network. These values are then treated as generic markers to fit a Cox regression. The neural networks are typically trained to return a single value classifying inputs by whether an event occurs within a time horizon or not. This approach is simple to implement and can easily add or account for covariates in the Cox regression stage but must handle data censoring.

*Deep-Survival*: The second approach trains neural networks with survival-specific loss functions to generate survival curves directly. We evaluate four such approaches from the PyCox[20] package, chosen for their variety and standard implementation:

- DeepSurv[21] models *log-risk* as a *time-constant, proportional, non-linear* function
- LogisticHazard (LH)[22] models *log-risk* as a *time-varying, non-proportional, non-linear* function and attempts to eliminate batch size effects.
- MTLR[23] models *risk* with a *time-varying, non-proportional, logistic regression on a non-linear* function
- DeepHit[24] models *risk* as a *time-varying, non-proportional, non-linear* function and allows for several competing risks

## AI-ECG survival models

Several recent studies predict mortality from ECGs. These are either built completely on large, private, ECG banks[3,4,5,10,16,25] or are fine-tuned in the context of a particular setting or population[2,11,12]. Some studies use Deep-Survival[3,10,11], and some use Classifier-Cox approaches[4,5,25]. Most studies use a convolutional network to interpret ECG, with a slightly-more-popular choice being the Resnet architecture from Ribeiro et al.[5,10,17,25].

## Benchmarking Overview

Benchmark settings are summarized in (Table 2). We build a total of 554 models. We use two Convolutional Neural Network (CNN) architectures: InceptionTime[26] and a modified Resnet architecture[15]. For each architecture, we train four Deep-Survival models[21] and four Classifier-Cox models where neural net classifiers predict mortality up to one, two, five, and ten-year horizons. Models are trained with and without demographic data and compared to models trained only on demographic data via XGBoost or a simple feedforward network ('FF'). Additional model training and survival analysis details are in **the supplement**.

We make this resource publicly available at [github.com/cavalab/ecg-survival-benchmark](https://github.com/cavalab/ecg-survival-benchmark).

Table 2

Setting	Values
Survival Analysis	
Deep-Survival Models	DeepHit, DeepSurv, LogisticHazard, Multi-Task Logistic Regression
Classifier-Cox Models	Classifiers model mortality as binary at 1,2,5,10-yr horizons
ECG Deep Learning Architecture	InceptionTime, Resnet
Demographic options	None, Age + Sex, Age + Sex + ECG Machine Measure (MIMIC-IV only)*
Demographic-Only models	XGBoost, Feedforward Network*
Normalization	z-score per channel, based on model's training data

\* Three random seeds, five everywhere else

Table 2. Sweep parameters.

Figure 1

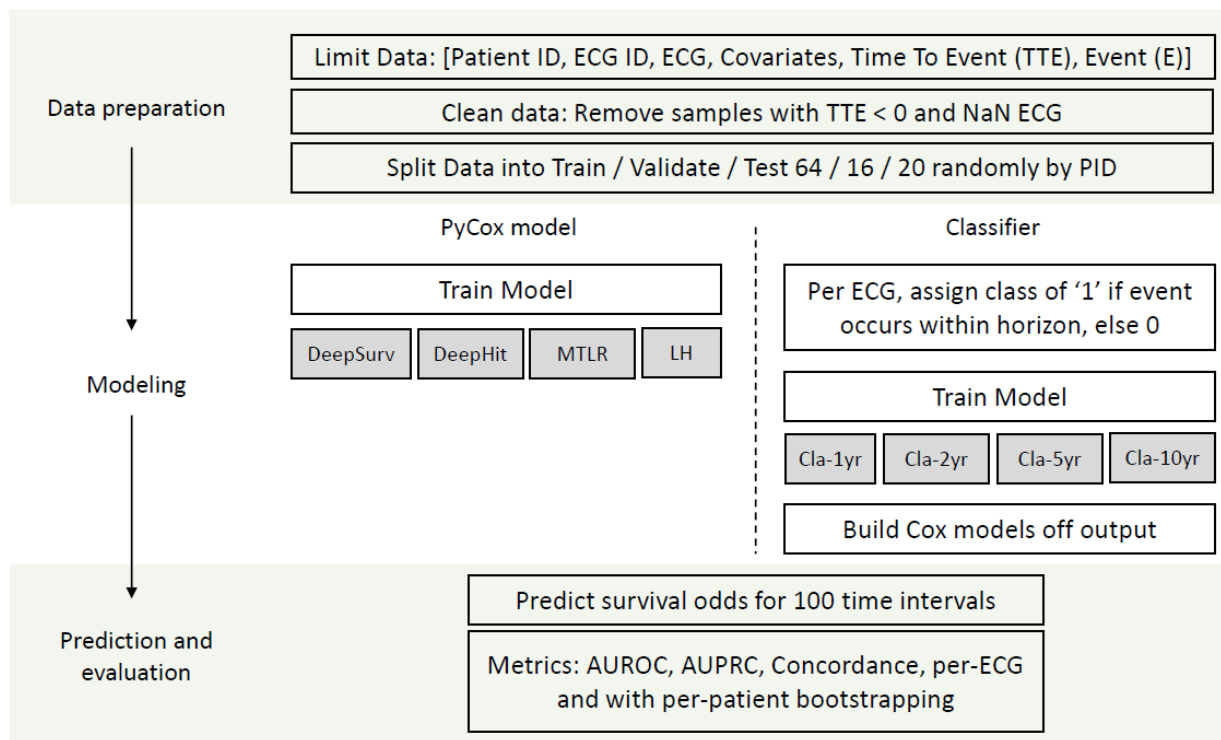


Figure 1. A diagram of the modeling process from data preparation to model evaluation

## Neural Network Structure

Our neural networks had three pieces: an ECG-processing piece, a demographic-processing piece (three feedforward-ReLU layers with output dimension 32), and a fusion piece connecting the other two pieces (three feedforward-ReLU layers with output dimension 128) that heads into a final linear layer (dimension 1 for Classifier-Cox models and DeepSurv, dimension 100 for LH, MTLR, and DeepHit – one per time bin). When demographic data is not included, the demographic-processing piece is skipped. When ECG is not included (for demographics-only baselines), the ECG piece returns a single dimension with a value of ‘0’, resulting in a feed-forward network.

We benchmark two ECG-processing architectures:

- “Resnet” is a multi-channel time series[15,25] adaptation of the original ResNet[27]. Architecture parameters were kept at defaults tuned to the full Code dataset. This model has 6.9-7.5M parameters.
- “InceptionTime”[26] adapts AlexNet[28] by widening convolutional kernel widths and including channel-wise bottlenecks to control model complexity. This architecture performs well on many small time-series classification benchmarks and has recently been used in fetal heart rate monitoring[29]. Architecture parameters were kept at the original publication’s defaults (kernel widths 11, 21, 41). This model has 510-530k parameters.

## Measures

Our primary metric is the Concordance Index (Concordance or C-Index). Concordance evaluates subject risk ordering: at the time of an event, a subject should be at a higher risk than any other subject still under observation; Concordance is the fraction of correctly ranked subject-subject comparisons.

## Statistics

Unless otherwise mentioned, paired comparisons use the Wilcoxon test and unpaired comparisons use the Mann-Whitney test. Multiple comparisons were adjusted for with Benjamini-Hochberg corrections at the 5% false discovery rate level.

# Results

## Public Dataset Modeling Results

Concordance indices across model sweeps are shown in **(Figure 2)**. Concordances for the top performing architecture, ResNet LogisticHazard, which ranked 2<sup>nd</sup> in Code-15 and 1<sup>st</sup> in MIMIC-IV, were (median; with Demographics - Code-15: 0.82, MIMIC-IV: 0.78; without Demographics - Code-15: 0.80, MIMIC-IV: 0.77). Top-performing demographic-only models yield Concordances of 0.79 for Code-15 (FF Cla-2) and 0.66 for MIMIC-IV (FF Cla-2). Top-performing MIMIC-IV demographics-and-machine-measure models yielded Concordances of 0.73 (XGB Cla-1). The ResNet LogisticHazard ECG-and-demographics-and-machine-measure MIMIC-IV model yielded Concordance 0.77.

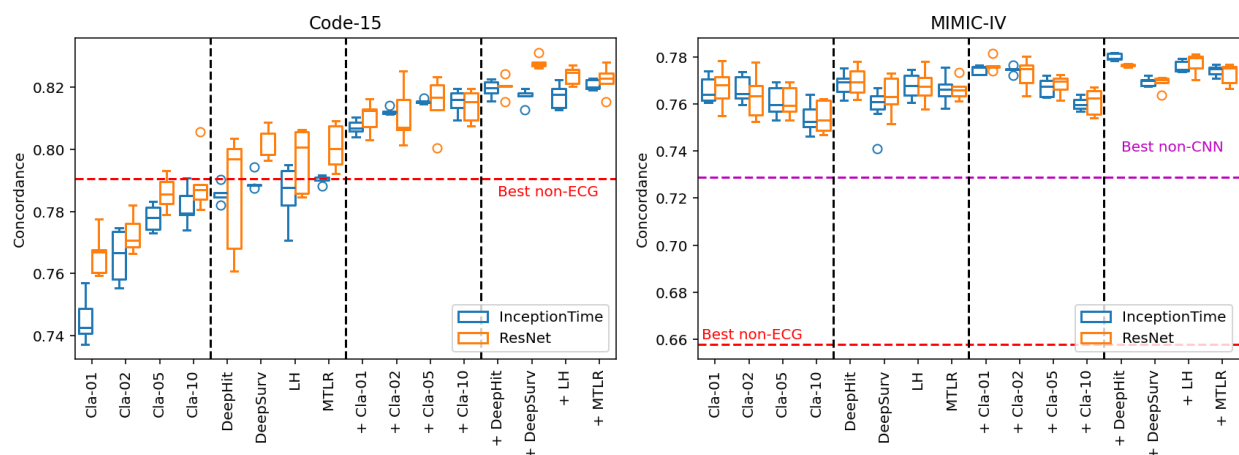


**Figure 2.** Model concordances across data, demographic inclusion, architecture, and survival modeling approaches. ‘+’: model trained with age/sex. Cla-H marks H-year horizon Classifier-Cox models. N=5 per configuration. Best non-CNN is a MIMIC-IV XGB Cla-1 model trained on demographics and automatic ECG machine measures (e.g. QRS).

Resnet Models, overall, show statistically higher Concordance than InceptionTime in Code-15 cases (median; ECG-only: 0.79 vs 0.78,  $p=1.32E-5$ , with demographics: 0.818 vs 0.816,  $p=2.08E-2$ ) (**Supplemental Table 1**). This is expected as Resnet architectures are tuned to this case.

Deep Survival models, overall, show statistically higher Concordance than Classifier-Cox models for ECG-based models with both datasets whether demographics are included (median; Code-15: 0.821 vs 0.813,  $p<1E-5$ ; MIMIC-IV: 0.774 vs 0.769,  $p=9.00E-4$ ) or not (median; Code-15: 0.792 vs 0.773,  $p<1E-5$ ; MIMIC-IV: 0.763 vs 0.758,  $p=5.88E-5$ ) (**Supplemental table 1**). In demographic-only MIMIC models, Classifier-Cox approaches show statistically, but not substantively, higher performance than Deep Survival models (0.656 vs 0.654,  $p<1E-5$ ); notably, these Deep-Survival models did not include the winning XGB approach.

The choice of time horizon for training Classifier-Cox models significantly correlates with Concordance for both datasets, whether demographics are included (medians; Code-15: 0.35,  $p=0.025$ ; MIMIC-IV: -0.84,  $p<1E-5$ ) or not (median; Code-15: 0.69,  $p<1E-5$ ; MIMIC-IV: -0.80  $p<1E-5$ )

(**Supplemental Table 2**). The direction of this effect is positive in Code-15 and negative in MIMIC-IV (**Figure 2**), highlighting the difficulty of choosing an appropriate value that is generally applicable.

Models incorporating ECG and Demographics show significantly higher Concordance than ECG-only models (median; Code-15: 0.817 vs 0.783,  $p < 1E-5$ ; MIMIC-IV: 0.772 vs 0.760,  $p < 1E-5$ ) (**Supplemental Table 3**).

Further analysis of time-censored and per-patient Concordance, as well as AUROC and AUPRC, is in **Supplements**. The most concordant approach, ResNet LogisticHazard, shows higher AUPRC than demographic-only models or chance. We highlight median AUPRC at 1-year (ECG+Age+Sex / Age+Sex / Chance %; Code-15: 0.07 / 0.04 / 1.2%; MIMIC-IV: 0.45 / 0.25 / 14.8%; BCH: 0.04 / 0.02 / 0.9%) and 5-years (ECG+Age+Sex / Age+Sex / Chance %; Code-15: 0.14 / 0.11 / 3.4%; MIMIC-IV: 0.55 / 0.42 / 24.5%; BCH: 0.13 / 0.07 / 4.8%).

We compare Kaplan-Meier curves for BCH and Code-15 to mean predicted population survival from ECG-only models in **Supplemental Figure 1**, confirming that model estimates generally follow the data. We also investigate model explainability with a media-waveform analysis[8] in **Supplemental Figure 2**; this highlighted dampened QRS activity, indicative of LV dysfunction, in high-risk patients.

## External Validation

We evaluated model ability to generalize to new sites in **Table 3**. Models generally perform best on their respective test sets, as expected. Models trained on BCH and MIMIC-IV transferred poorly to Code-15, exemplified by a 0.24 drop in BCH model concordance. Demographic-only survival models provide a strong baseline for the Code-15 cohort, even when trained externally; e.g., the best demographic-only model trained on MIMIC-IV shows a concordance of 0.79 on Code-15, which matches a Code-15-trained, ECG-only model. All Code-15 and MIMIC-IV ECG models perform better than demographic-only models on BCH (0.73/0.75, respectively), and transfer the best overall between sites. We further evaluated model performance on patient subgroups in **Supplemental Figure 3**, but did not find that model performance differentials between sites was sufficiently explained by differences in age and sex among cohorts.

Concordance (higher better)		ResNet LogisticHazard						Best** Non-ECG model			
		ECG			ECG + Age/Sex			Median	25%	75%	Approach
Test Data	Training Data	Median	25%	75%	Median	25%	75%	Median	25%	75%	Approach
BCH	BCH	0.77	0.76	0.77	0.76	0.76	0.76	0.67	0.66	0.67	FF DeepHit
	Code15	0.74	0.74	0.74	0.73	0.73	0.74	0.65	0.65	0.65	
	MIMICIV	0.71	0.69	0.71	0.75	0.73	0.75	0.65	0.65	0.65	
Code15	BCH	0.53	0.51	0.54	0.54	0.54	0.55	0.77	0.77	0.78	FF CLA-2
	Code15	0.80	0.79	0.81	0.82	0.82	0.83	0.79	0.79	0.79	
	MIMICIV	0.62	0.62	0.65	0.70	0.68	0.70	0.79	0.79	0.79	
MIMICIV	BCH	0.65	0.64	0.66	0.65	0.62	0.65	0.65	0.65	0.65	FF CLA-2
	Code15	0.70	0.68	0.70	0.71	0.70	0.71	0.66	0.66	0.66	
	MIMICIV*	0.77	0.76	0.77	0.78	0.78	0.78	0.66	0.66	0.66	

\* with Age/Sex/Machine measures: ResNet LogisticHazard: 0.78; 0.73 with XGB CLA-1  
 \*\* Best by median concordance on Training Data's corresponding Test Set (ex: BCH/BCH)

Table 3. ‘ResNet LogisticHazard’ ranked 1<sup>st</sup> for ‘ECG + Age/Sex’ in MIMIC-IV and 2<sup>nd</sup> in Code-15 and was used for BCH survival models. These models were then evaluated on all datasets. Color-coding is per Test dataset; Red: lowest, Blue: highest, White: local Non-ECG. FF- feedforward.

## Discussion and Conclusions

This work is the first to comprehensively benchmark survival modeling approaches in all-cause mortality prediction on the public Code-15 and MIMIC-IV datasets, and evaluate the resultant models in a pediatric setting. We provide verifiable results and baselines that inform future model development (ECG-processing approaches, survival analysis approaches). We also release our code, which can be adapted to evaluate new modeling approaches or used to train AI-ECG survival-analysis models. While classification-based mortality modeling allows for some patient risk stratification, survival-analysis modeling is broader in that it models event occurrence (e.g. diagnostic threshold crossing) from data in the [time-to-event, event] format. Applied carefully to a patient subgroup, this could inform decisions on patient care or logistics (e.g. scheduling) in finer detail.

### Demographic-Only models

Studies rarely compare AI-ECG to simpler models such as demographic-only models. AI-ECG’s value depends on its favorable performance against these competitors. Here, we find that this value is sometimes small and varies substantially with dataset, suggesting ECG-based models may add more value in acute settings (BCH, MIMIC-IV) than in out-patient settings (Code-15).

### Model Generalizability

Models trained on MIMIC-IV and Code-15 transferred better to BCH than vice versa. This difference is not explained by age or sex related performance differences (Supplemental Figure 3), and isn’t attributable purely to differences in mortality rates (4/28/7% for Code-15/MIMIC-IV/BCH, respectively, Table 1). We conjecture these differences arise from multiple factors related to the care setting and cohort differences between these sites. Whereas future work may tease apart additional explanations, the results suggest that site-specific models are likely to perform significantly better than an externally trained AI-ECG model; in some cases (Code-15), even simple demographic models appear to transfer better.

### Comparisons to past work

Our results match past studies which predict mortality at the one-year mark (0.81-0.85 Concordance)[4,5] and five-year mark (0.78-0.83 Concordance)[1,5]. Additionally, our ResNet DeepHit ECG-only MIMIC-IV results (0.769 Concordance) match a recent study (0.775 Concordance) that trained a ResNet DeepHit model, AIRE[10], on 1.2M ECGs from Beth-Israel Deaconess Medical Center in Boston, MA. We expect this dataset to substantially overlap with MIMIC-IV.

Past work reports insubstantial performance drops across similar cohorts[1] and AIRE[10] reports Concordance drops of 0.01-0.13 on different cohorts. Although AIRE’s 0.762 Concordance on the full Code dataset improves on our ECG-only CNN models’ 0.62, both are lower than a Code-15

demographics-only model (0.79). This again suggests that models should be tested against, and calibrated to, local baselines.

## On survival modeling approaches

We recommend Deep-Survival approaches since they perform more reliably than Classifier-Cox models and limit data censoring problems.

*Performance.* On average, Deep-Survival models increase Concordance by 0.005-0.02 over Classifier-Cox models. For Code-15, this is substantial when comparing AI-ECG models to demographic-only models (median Concordance 0.821 / 0.813 / 0.789 for Deep-Survival / Classifier-Cox / demographic-only models). For MIMIC-IV, this is substantial when comparing newer, CNN-based, models to older feature-based models (median Concordance 0.774 / 0.769 / 0.729 for Deep-Survival / Classifier-Cox / demographic-and-machine-measure models). See **Supplemental Analysis** for performance tables.

*Data Censoring – Horizon.* In Classifier-Cox models, horizon choice affects performance. Short-horizon data includes few positive-event samples but assumptions about censored patients have little effect. Long-horizon data has more positive-event samples but the assumptions about censored patients have time to compound. Our results indicate that horizon choice is both dataset-specific, with opposing trends for Code-15 and MIMIC-IV, and substantial.

*Data Censoring – Labels.* When training classifiers, we label events as a ‘1’ when patients experience an event by horizon  $h$ , else 0, even if censored. This same labeling applied to AUROC/PRC, but not Concordance. While there is no standard approach for integrating censored patients with time-dependent measures[30], past work tends to exclude patients that have not reached the horizon-of-interest[4,5], which inflates the event rate (imagine a 1000-person study with an annual 90 percent drop-out rate and 1 percent event rate: after two years there are 11 events and 8 remaining controls). We chose to mark censored patients as non-events for classifier labels and AUROC/PRC to avoid inflating the event rate. This is reasonable for Code-15, where drop-out rates exceed event rates, and for MIMIC-IV, where censoring indicates lower patient risk.

## Limitations

First, architectures are limited to those vetted for “long” physiological time-series. Second, while many papers tune model architectures specifically for their datasets, we did not and cannot provide guidance for architecture modifications. Third, past work typically evaluates model performance per pathology. Doing so requires expert input and dataset standardization across multiple databases, which is beyond the scope of this work. The ethical deployment of survival models in a clinical setting requires that model performance be evaluated in those contexts with appropriate subgroup analyses, oversight, and a focus on how model use impacts patient care.

## Conclusions

We benchmark mortality prediction from ECGs with two CNN architectures on the two largest public ECG datasets using four Deep-Survival models and four Classifier-Cox regressions, and then extend the best configuration to a private ECG dataset. Our results highlight the importance of demographic-only baselines, the benefits of including demographics in AI-ECG modeling, and the

benefits of Deep-Survival models over Classifier-Cox approaches. Cross-dataset evaluation shows large performance drops and implies that model generalization is not guaranteed. Our results are reasonable given past studies and the event rates per dataset. We hope this provides a valuable resource for future ECG and ECG-mortality studies.

## Acknowledgments and Funding Disclosures

### Author Contributions

- Platon Lukyanenko: investigation, formal analysis, writing - original draft, figures
- Joshua Mayourian: data curation, conceptualization, methodology
- Mingxuan Liu: data curation, figures
- John K. Triedman: conceptualization, methodology
- Sunil J. Ghelani: conceptualization, methodology
- William G. La Cava: methodology, resources, investigation, supervision, project administration
- All authors: writing- review & editing.

### Computing Sorces

The authors would like to acknowledge Boston Children’s Hospital’s High-Performance Computing Resources Clusters Enkefalos 2/3 (E2/3) made available for conducting the research reported in this publication.

### Funding Sources

Funding support received from the Thrasher Research Fund Early Career Award (J.M.), Boston Children’s Hospital Electrophysiology Research Education Fund (J.M., J.K.T.), NIH grant R00-LM012926 from the National Library of Medicine (W.G.L.), NIH grant T32HD040128 from the National Institute of Childhood Diseases and Human Development (P.L.), and the Kosten Innovation Fund (W.G.L.).

### Data Sharing

Dataset Licenses The MIMIC-IV ECG dataset is available from <https://physionet.org/content/mimic-iv-ecg/1.0/> under the Open Data Commons Open Database License v1.0. The Code-15 dataset is available from <https://zenodo.org/records/4916206> under Creative Commons license CC-BY 4.0. The datasets use de-identified patient information. The BCH data is restricted; researchers can contact the corresponding author to coordinate data-sharing agreements between institutions. Code to reproduce the experiments is available from <https://github.com/cavalab/ecg-survival-benchmark> under a GNU Public License version 3.0.

## References

- [1] J. Weston Hughes, James Tooley, Jessica Torres Soto, Anna Ostropolets, Tim Poterucha, Matthew Kai Christensen, Neal Yuan, Ben Ehlert, Dhamanpreet Kaur, Guson Kang, Albert Rogers, Sanjiv Narayan, Pierre Elias, David Ouyang, Euan Ashley, James Zou, and Marco V. Perez. A deep learning-based electrocardiogram risk score for long term cardiovascular death and disease. *npj Digital Medicine*, 6(1):169, September 2023. 2, 5, 8
- [2] Salah S. Al-Zaiti, Christian Martin-Gill, Jessica K. Zègre-Hemsey, Zeineb Bouzid, Ziad Faramand, Mohammad O. Alrawashdeh, Richard E. Gregg, Stephanie Helman, Nathan T. Riek, Karina Kraevsky-Phillips, Gilles Clermont, Murat Akcakaya, Susan M. Sereika, Peter Van Dam, Stephen W. Smith, Yochai Birnbaum, Samir Saba, Ervin Sejdic, and Clifton W. Callaway. Machine learning for ECG diagnosis and risk stratification of occlusion myocardial infarction. *Nature Medicine*, 29(7):1804–1813, July 2023. 1, 2, 3
- [3] Shaan Khurshid, Samuel Friedman, Christopher Reeder, Paolo Di Achille, Nathaniel Diamant, Pulkit Singh, Lia X. Harrington, Xin Wang, Mostafa A. Al-Alusi, Gopal Sarma, Andrea S. Foulkes, Patrick T. Ellinor, Christopher D. Anderson, Jennifer E. Ho, Anthony A. Philippakis, Puneet Batra, and Steven A. Lubitz. ECG-Based Deep Learning and Clinical Risk Factors to Predict Atrial Fibrillation. *Circulation*, 145(2):122–133, January 2022. 3
- [4] Sushravya Raghunath, Alvaro E. Ulloa Cerna, Linyuan Jing, David P. vanMaanen, Joshua Stough, Dustin N. Hartzel, Joseph B. Leader, H. Lester Kirchner, Martin C. Stumpe, Ashraf Hafez, Arun Nemani, Tanner Carbonati, Kipp W. Johnson, Katelyn Young, Christopher W. Good, John M. Pfeifer, Aalpen A. Patel, Brian P. Delisle, Amro Alsaïd, Dominik Beer, Christopher M. Haggerty, and Brandon K. Fornwalt. Prediction of mortality from 12-lead electrocardiogram voltage data using a deep neural network. *Nature Medicine*, 26(6):886–891, June 2020. 2, 3, 8
- [5] Weijie Sun, Sunil Vasu Kalmady, Nariman Sepehrvand, Amir Salimi, Yousef Nademi, Kevin Baine, Justin A. Ezekowitz, Russell Greiner, Abram Hindle, Finlay A. McAlister, Roopinder K. Sandhu, and Padma Kaul. Towards artificial intelligence-based learning health system for population-level mortality prediction using electrocardiograms. *npj Digital Medicine*, 6(1):21, February 2023. 1, 2, 3, 8
- [6] Takahiro Kokubo, Satoshi Kodera, Shinnosuke Sawano, Susumu Katsushika, Mitsuhiro Nakamoto, Hirotochi Takeuchi, Nisei Kimura, Hiroki Shinohara, Ryo Matsuoka, Koki Nakanishi, Tomoko Nakao, Yasutomi Higashikuni, Norifumi Takeda, Katsuhito Fujiu, Masao Daimon, Hiroshi Akazawa, Hiroyuki Morita, Yutaka Matsuyama, and Issei Komuro. Automatic detection of left ventricular dilatation and hypertrophy from electrocardiograms using deep learning. *International Heart Journal*, 63(5):939–947, 2022. 1
- [7] Demilade Adedinsewo, Rickey E. Carter, Zachi Attia, Patrick Johnson, Anthony H. Kashou, Jennifer L. Dugan, Michael Albus, Johnathan M. Sheele, Fernanda Bellolio, Paul A. Friedman, Francisco Lopez-Jimenez, and Peter A. Noseworthy. Artificial Intelligence-Enabled ECG Algorithm to Identify Patients With Left Ventricular Systolic Dysfunction Presenting to the Emergency Department With Dyspnea. *Circulation: Arrhythmia and Electrophysiology*, 13(8):e008437, August 2020. Publisher: American Heart Association. 1

- [8] Joshua Mayourian, William G. La Cava, Akhil Vaid, Girish N. Nadkarni, Sunil J. Ghelani, Rebekah Mannix, Tal Geva, Audrey Dionne, Mark E. Alexander, Son Q. Duong, and John K. Triedman. Pediatric ECG-Based Deep Learning to Predict Left Ventricular Dysfunction and Re-modeling. *Circulation*, 149(12):917–931, March 2024. Publisher: American Heart Association.1
- [9] Hongling Zhu et al. Four-Channel ECG as a Single Source for Early Diagnosis of Cardiac Hypertrophy and Dilation — A Deep Learning Approach. *NEJM AI* 2024-09-26
- [10] Artificial intelligence-enabled electrocardiogram for mortality and cardiovascular risk estimation: a model development and validation study. Sau, Arunashis et al. *The Lancet Digital Health*, Volume 6, Issue 11, e791 - e802
- [11] R. R. Van De Leur, H. Bleijendaal, K. Taha, T. Mast, J. M. I. H. Gho, M. Linschoten, B. Van Rees, M. T. H. M. Henkens, S. Heymans, N. Sturkenboom, R. A. Tio, J. A. Offerhaus, W. L. Bor, M. Maarse, H. E. Haerkens-Arends, M. Z. H. Kolk, A. C. J. Van Der Lingen, J. J. Selder, E. E. Wierda, P. F. M. M. Van Bergen, M. M. Winter, A. H. Zwinderman, P. A. Doevendans, P. Van Der Harst, Y. M. Pinto, F. W. Asselbergs, R. Van Es, F. V. Y. Tjong, and the CAPACITY- COVID collaborative consortium. Electrocardiogram-based mortality prediction in patients with COVID-19 using machine learning. *Netherlands Heart Journal*, 30(6):312–318, June 2022.2, 3
- [12] Kuba Weimann and Tim O. F. Conrad. Transfer learning for ECG classification. *Scientific Reports*, 11(1):5251, March 2021. Publisher: Nature Publishing Group. 2
- [13] Brian Gow, Tom Pollard, Larry A Nathanson, Alistair Johnson, Benjamin Moody, Chrystinne Fernandes, Nathaniel Greenbaum, Jonathan W Waks, Parastou Eslami, Tanner Carbonati, Ashish Chaudhari, Elizabeth Herbst, Dana Moukheiber, Seth Berkowitz, Roger Mark, and Steven Horng. MIMIC-IV-ECG: Diagnostic Electrocardiogram Matched Subset, 2023. 1, 2, 3
- [14] A. L. Goldberger, L. A. N. Amaral, L. Glass, J. M. Hausdorff, P. Ch. Ivanov, R. G. Mark, J. E. Mietus, G. B. Moody, C.-K. Peng, and H. E. Stanley. PhysioBank, PhysioToolkit, and PhysioNet: Components of a new research resource for complex physiologic signals. *Circulation*, 101(23):e215–e220, 2000 (June 13). *Circulation Electronic Pages*: <http://circ.ahajournals.org/content/101/23/e215.full> PMID:1085218; doi: 10.1161/01.CIR.101.23.e215.
- [15] Antônio H. Ribeiro, Manoel Horta Ribeiro, Gabriela M. M. Paixão, Derick M. Oliveira, Paulo R. Gomes, Jéssica A. Canazart, Milton P. S. Ferreira, Carl R. Andersson, Peter W. Macfarlane, Wagner Meira, Thomas B. Schön, and Antonio Luiz P. Ribeiro. Automatic diagnosis of the 12-lead ECG using a deep neural network. *Nature Communications*, 11(1):1760, April 2020. 1, 2, 3, 4, 5, 7
- [16] Elena Merdjanovska and Aleksandra Rashkovska. Comprehensive survey of computational ECG analysis: Databases, methods and applications. *Expert Systems with Applications*, 203:117206, October 2022. 2
- [17] Joshua Mayourian, Amr El-Bokl, Platon Lukyanenko, William G La Cava, Tal Geva, Anne Marie Valente, John K Triedman, Sunil J Ghelani, Electrocardiogram-based deep learning to predict mortality in paediatric and adult congenital heart disease, *European Heart Journal*, 2024;, ehae651, <https://doi.org/10.1093/eurheartj/ehae651>

- [18] David R Cox. Regression models and life-tables. *Journal of the Royal Statistical Society: Series B (Methodological)*, 34(2):187–202, 1972. 2
- [19] Terry M. Therneau. Modeling survival data: Extending the Cox Model. In P. Bickel, P. Diggle, S. Fienberg, K. Krickeberg, I. Olkin, N. Wermuth, S. Zeger, D. Y. Lin, and T. R. Fleming, editors, *Proceedings of the First Seattle Symposium in Biostatistics*, volume 123, pages 51–84. Springer US, New York, NY, 1997. 2
- [20] Håvard Kvamme, Ørnulf Borgan, and Ida Scheel. Time-to-Event Prediction with Neural Networks and Cox Regression. *Journal of Machine Learning Research*, 20(129):1–30, 2019. 3, 5
- [21] Jared L. Katzman, Uri Shaham, Alexander Cloninger, Jonathan Bates, Tingting Jiang, and Yuval Kluger. DeepSurv: personalized treatment recommender system using a Cox proportional hazards deep neural network. *BMC Medical Research Methodology*, 18(1):24, December 2018. 3, 5
- [22] Michael F. Gensheimer and Balasubramanian Narasimhan. A scalable discrete-time survival model for neural networks. *PeerJ*, 7:e6257, January 2019. 3, 5
- [23] Stephane Fotso. Deep Neural Networks for Survival Analysis Based on a Multi-Task Framework, January 2018. arXiv:1801.05512[cs, stat]. 3, 5
- [24] Changhee Lee, William Zame, Jinsung Yoon, and Mihaela Van Der Schaar. DeepHit: A Deep Learning Approach to Survival Analysis With Competing Risks. *Proceedings of the AAAI Conference on Artificial Intelligence*, 32(1), April 2018. 3, 5
- [25] Emilly M. Lima, Antônio H. Ribeiro, Gabriela M. M. Paixão, Manoel Horta Ribeiro, Marcelo M. Pinto-Filho, Paulo R. Gomes, Derick M. Oliveira, Ester C. Sabino, Bruce B. Duncan, Luana Giatti, Sandhi M. Barreto, Wagner Meira Jr, Thomas B. Schön, and Antonio Luiz P. Ribeiro. Deep neural network-estimated electrocardiographic age as a mortality predictor. *Nature Communications*, 12(1):5117, August 2021. 3, 4
- [26] Hassan Ismail Fawaz, Benjamin Lucas, Germain Forestier, Charlotte Pelletier, Daniel F. Schmidt, Jonathan Weber, Geoffrey I. Webb, Lhassane Idoumghar, Pierre-Alain Muller, and François Petitjean. InceptionTime: Finding AlexNet for Time Series Classification. *Data Mining and Knowledge Discovery*, 34(6):1936–1962, November 2020. arXiv:1909.04939[cs, stat]. 3, 4, 5
- [27] Kaiming He, Xiangyu Zhang, Shaoqing Ren, and Jian Sun. Deep Residual Learning for Image Recognition. In *2016 IEEE Conference on Computer Vision and Pattern Recognition (CVPR)*, pages 770–778, June 2016. 4
- [28] Alex Krizhevsky, Ilya Sutskever, and Geoffrey E Hinton. ImageNet Classification with Deep Convolutional Neural Networks. In *Advances in Neural Information Processing Systems*, volume 25. Curran Associates, Inc., 2012. 4
- [29] Jennifer A. McCoy, Lisa D. Levine, Guangya Wan, Corey Chivers, Joseph Teel, and William G. La cava. Intrapartum electronic fetal heart rate monitoring to predict acidemia at birth with the use of deep learning. *American Journal of Obstetrics and Gynecology*, April 2024. 4
- [30] Terry M Therneau. A Package for Survival Analysis in R, 2024. R package version 3.6-4. 5 [38] Adina Najwa Kamarudin, Trevor Cox, and Ruwanthi Kolamunnage-Dona. Time-dependent ROC

## Supplements

### Additional Modeling Details

#### Model Training

Models train for up to 200 epochs, stopping early if their performance on the validation set does not improve for 20 consecutive epochs. As in past work[1], we use the AdamW optimizer, start with a  $1e-3$  learning rate, and scale the learning rate by  $0.1x$  if validation performance does not improve for 10 consecutive epochs to a minimum of  $1e-8$ [2]. We trained models with three random seeds for the (MIICIV + age + sex + machine measure) case and feedforward demographic models, and otherwise used five random seeds. Models were trained on a cluster that unpredictably provided a A40, A100, L40 or Nvidia Quadro GPU. Data was loaded to RAM, requesting 100GB for Code-15, 150GB for BCH, and 300GB for MIMIC-IV. Training was done on batches of 512 shuffled data samples with 256 loaded onto a GPU concurrently. Per configuration, we evaluate the model with minimum validation loss.

Additionally, DeepSurv requires GPU batches to contain positive events for loss calculations; for these models, GPU-batches that contained no positive-event samples had their last sample replaced with a positive-event sample chosen randomly from the training set.

Code-15 models averaged 4.5 hours to train and achieved maximum validation performance by 30 epochs. MIMIC-IV models took 7.2 hours and achieved maximum validation performance by 12 epochs. Training times depend on GPU, with faster GPUs taking 600s/epoch and slower ones up to 2200s/epoch. GPU batch sizes were based on slower GPUs.

#### Survival Modeling

Concordance is measured with the Antolini Concordance[3] implementation from PyCox with score contributions weighted by Kaplan-Meier estimates.

For Classifier-Cox models, the classifier's output is a binary label predicting mortality by a time horizon. We treat this output as a generic biomarker and fit a Cox regression on validation data with the scikit-survival package[4-6]. This fitting step includes the full[time-to-event, event] information, so these regressions still model mortality over the full dataset's timespan.

The LH, MTLR, and DeepHit models fit survival functions at discrete time points. We used 100 uniformly distributed time points between '0' and the maximum time-to-event in each validation dataset. DeepSurv models and Cox regressions can be queried at any time of interest.

Before measuring model performance, to maintain consistency, we sample the Cox and DeepSurv survival functions at the same 100 time points used to fit the LH, MTLR, and DeepHit models. This

sampling greatly simplifies Concordance calculations, which would otherwise need survival estimates for every ECG at every unique time-to-event.

When measuring model performance at the 1,2,5,10-year marks, we use the temporally closest sampled survival function value (e.g. MIMIC-IV data has a maximum follow-up time of almost 13 years; one-year AUROC is measured from the survival function at the 1.008-year mark).

See[7] for a thorough guide to survival modeling.

## Section References

[1] J. Weston Hughes, James Tooley, Jessica Torres Soto, Anna Ostropolets, Tim Poterucha, Matthew Kai Christensen, Neal Yuan, Ben Ehlert, Dhamanpreet Kaur, Guson Kang, Albert Rogers, Sanjiv Narayan, Pierre Elias, David Ouyang, Euan Ashley, James Zou, and Marco V. Perez. A deep learning-based electrocardiogram risk score for long term cardiovascular death and disease. *npj Digital Medicine*, 6(1):169, September 2023. 2, 5, 8

[2] Antônio H. Ribeiro, Manoel Horta Ribeiro, Gabriela M. M. Paixão, Derick M. Oliveira, Paulo R. Gomes, Jéssica A. Canazart, Milton P. S. Ferreira, Carl R. Andersson, Peter W. Macfarlane, Wagner Meira, Thomas B. Schön, and Antonio Luiz P. Ribeiro. Automatic diagnosis of the 12-lead ECG using a deep neural network. *Nature Communications*, 11(1):1760, April 2020. 1, 2, 3, 4, 5, 7

[3] Laura Antolini, Patrizia Boracchi, and Elia Biganzoli. A time-dependent discrimination index for survival data. *Statistics in Medicine*, 24(24):3927–3944, December 2005. 5

[4] Sebastian Pölsterl, Nassir Navab, and Amin Katouzian. Fast training of support vector machines for survival analysis. In Annalisa Appice, Pedro Pereira Rodrigues, Vítor Santos Costa, João Gama, Alípio Jorge, and Carlos Soares, editors, *Machine Learning and Knowledge Discovery in Databases, Lecture Notes in Computer Science*, pages 243–259, 2015. 5

[5] Sebastian Pölsterl, Gupta Pankaj, Lichao Wang, Sailesh Conjeti, Amin Katouzian, and Nassir Navab. Heterogeneous Ensembles for Predicting Survival of Metastatic, Castrate-Resistant Prostate Cancer Patients. *F1000Research*, 5(2676), November 2016.

[6] Sebastian Pölsterl, Nassir Navab, and Amin Katouzian. An Efficient Training Algorithm for Kernel Survival Support Vector Machines. In *3rd Workshop on Machine Learning in Life Sciences*, September 2016. 5

[7] D. Y. Lin. On the Breslow estimator. *Lifetime Data Analysis*, 13(4):471–480, December 2007. 2

## Supplement table 1

Code-15 Concordance												
		ECG			ECG + Demographic			Demographic models				
N	Category	median	25th	75th	median	25th	75th	N	Type	median	25th	75th
40	Classifier-Cox	0.773	0.767	0.783	0.813	0.808	0.816	32	XGB/FF	0.789	0.787	0.791
40	Deep-Survival	0.792	0.787	0.800	0.821	0.818	0.824	12	FF	0.790	0.790	0.790
Mann-Whitney P value		<b>7.99E-09</b>			<b>3.56E-09</b>			1.59E-01				
40	InceptionTime	0.778	0.773	0.788	0.816	0.813	0.819					
40	Resnet	0.788	0.777	0.800	0.818	0.813	0.825					
Wilcoxon P value		<b>1.32E-05</b>			<b>2.08E-02</b>							

MIMIC-IV Concordance												
		ECG			ECG + Demographic			Demographic models				
N	Category	median	25th	75th	median	25th	75th	N	Type	median	25th	75th
40	Classifier-Cox	0.758	0.753	0.763	0.769	0.763	0.775	32	XGB/FF	0.656	0.655	0.658
40	Deep-Survival	0.763	0.761	0.767	0.774	0.771	0.777	12	FF	0.654	0.653	0.654
Mann-Whitney P value		<b>5.88E-05</b>			<b>9.00E-04</b>			<b>4.50E-07</b>				
40	InceptionTime	0.760	0.758	0.764	0.772	0.769	0.776					
40	Resnet	0.760	0.756	0.765	0.772	0.769	0.776					
Wilcoxon P value		9.60E-01			9.40E-01							

Supplemental Table 1. Comparisons between Classifier-Cox and Deep-Survival, and between InceptionTime and ResNet, for Code-15 and MIMIC-IV.

## Supplement table 2

Classifier Horizon vs Concordance				
Dataset	ECG + Demographic		ECG Only	
	Pearson R	P value	Pearson R	P value
Code-15	0.35	<b>2.49E-02</b>	0.69	<b>8.12E-07</b>
MIMIC-IV	-0.8377	<b>1.57E-11</b>	-0.8	<b>5.49E-10</b>

Supplemental Table 2. Concordance Index correlates with classifier horizon in Code-15 and MIMIC-IV whether demographics are included or not.

## Supplement Table 3

ECG vs ECG + Demographics					
Dataset	Data Types	N	median	25th	75th
Code-15	ECG	80	0.783	0.743	0.808
	ECG+Age+Sex	80	0.817	0.803	0.828
	Wilcoxon P value			<b>7.85E-15</b>	
MIMIC-IV	ECG	80	0.760	0.757	0.765
	ECG+Age+Sex	80	0.772	0.769	0.776
	Wilcoxon P value			<b>7.85E-15</b>	

Supplemental Table 3. Code-15 and MIMIC-IV Models that include Age/Sex perform better than models that do not.

## Supplemental Analysis

Concordance is usually measured across all time points, although some authors suggest that endpoints are essential to proper model interpretation[36]. We include Concordance with event times censored to the one, two, five, and ten-year marks in **Supplemental Table 4**. The censoring determines which pairs are considered comparable. We also repeat this in a bootstrap manner, keeping only one ECG per subject in **Supplemental Table 5**.

We also measure AUPRC and AUROC, comparing cumulative hazard,  $H(T) = 1 - S(t)$ , to the ‘correct’ labels set just as in our classifier labeling (1 if a patient experiences an event by time T, else 0, even if censored), in **Supplemental Table 6**.

Supplement Table 4

Concordance (censored to year y), across all ECGs														
Data	Architecture	Model	Covariates	N	1-Yr	2-Yr	(25-75th%)	5-Yr	(25-75th%)	10-Yr	(25-75th%)	All-Time	(25-75th%)	
Code15	Ribeiro	DeepSurv	age, sex	5	0.8333	(0.8327, 0.8335)	0.8297	(0.8289, 0.8306)	0.8278	(0.8272, 0.8283)	0.8276	(0.8270, 0.8280)	0.8276	(0.8270, 0.8280)
Code15	Ribeiro	LH	age, sex	5	0.8335	(0.8256, 0.8347)	0.8274	(0.8205, 0.8281)	0.825	(0.8213, 0.8260)	0.8248	(0.8211, 0.8256)	0.8248	(0.8211, 0.8256)
Code15	Ribeiro	MTLR	age, sex	5	0.8266	(0.8240, 0.8289)	0.8223	(0.8218, 0.8258)	0.8229	(0.8213, 0.8247)	0.8227	(0.8212, 0.8244)	0.8227	(0.8212, 0.8244)
Code15	Ribeiro	DeepHit	age, sex	5	0.8237	(0.8236, 0.8258)	0.8206	(0.8195, 0.8222)	0.8207	(0.8206, 0.8207)	0.8206	(0.8204, 0.8206)	0.8206	(0.8204, 0.8206)
Code15	InceptionTime	MTLR	age, sex	5	0.8233	(0.8214, 0.8262)	0.8193	(0.8186, 0.8220)	0.8201	(0.8196, 0.8228)	0.8201	(0.8195, 0.8225)	0.8201	(0.8195, 0.8225)
Code15	InceptionTime	DeepHit	age, sex	5	0.8231	(0.8229, 0.8233)	0.8203	(0.8192, 0.8208)	0.8198	(0.8183, 0.8217)	0.8197	(0.8183, 0.8216)	0.8197	(0.8183, 0.8216)
Code15	InceptionTime	DeepSurv	age, sex	5	0.8181	(0.8162, 0.8191)	0.8165	(0.8162, 0.8188)	0.8181	(0.8170, 0.8182)	0.8181	(0.8172, 0.8182)	0.8181	(0.8172, 0.8182)
Code15	InceptionTime	LH	age, sex	5	0.82	(0.8151, 0.8250)	0.8183	(0.8114, 0.8188)	0.8176	(0.8134, 0.8198)	0.8176	(0.8133, 0.8196)	0.8176	(0.8133, 0.8196)
Code15	Ribeiro	Cla-5	age, sex	5	0.8212	(0.8183, 0.8261)	0.8163	(0.8138, 0.8224)	0.8166	(0.8126, 0.8209)	0.8166	(0.8128, 0.8207)	0.8166	(0.8128, 0.8207)
Code15	InceptionTime	Cla-10	age, sex	5	0.8167	(0.8131, 0.8195)	0.8151	(0.8117, 0.8169)	0.8161	(0.8134, 0.8183)	0.8161	(0.8135, 0.8182)	0.8161	(0.8135, 0.8182)
Code15	Ribeiro	Cla-10	age, sex	5	0.8185	(0.8131, 0.8232)	0.8174	(0.8094, 0.8176)	0.8156	(0.8092, 0.8181)	0.8154	(0.8093, 0.8181)	0.8154	(0.8093, 0.8181)
Code15	InceptionTime	Cla-5	age, sex	5	0.8177	(0.8176, 0.8180)	0.8148	(0.8140, 0.8153)	0.8152	(0.8150, 0.8156)	0.8151	(0.8150, 0.8155)	0.8151	(0.8150, 0.8155)
Code15	Ribeiro	Cla-1	age, sex	5	0.8262	(0.8182, 0.8314)	0.8151	(0.8083, 0.8184)	0.8129	(0.8073, 0.8135)	0.8125	(0.8072, 0.8129)	0.8125	(0.8072, 0.8129)
Code15	InceptionTime	Cla-2	age, sex	5	0.8139	(0.8136, 0.8145)	0.8109	(0.8104, 0.8120)	0.8118	(0.8115, 0.8122)	0.8121	(0.8115, 0.8122)	0.8121	(0.8115, 0.8122)
Code15	Ribeiro	Cla-2	age, sex	5	0.819	(0.8150, 0.8265)	0.8098	(0.8091, 0.8182)	0.8073	(0.8065, 0.8161)	0.807	(0.8064, 0.8159)	0.807	(0.8064, 0.8159)
Code15	InceptionTime	Cla-1	age, sex	5	0.8118	(0.8081, 0.8150)	0.806	(0.8057, 0.8087)	0.8067	(0.8060, 0.8086)	0.8067	(0.8058, 0.8086)	0.8067	(0.8058, 0.8086)
Code15	FeedForward	Cla-2	age, sex	3	0.7783	(0.7782, 0.7784)	0.7843	(0.7841, 0.7844)	0.7907	(0.7904, 0.7907)	0.7908	(0.7906, 0.7909)	0.7908	(0.7906, 0.7909)
Code15	Ribeiro	DeepSurv	none	5	0.8181	(0.8141, 0.8213)	0.8122	(0.8048, 0.8137)	0.8055	(0.7986, 0.8058)	0.8051	(0.7982, 0.8051)	0.8051	(0.7982, 0.8051)
Code15	Ribeiro	LH	none	5	0.8181	(0.8007, 0.8271)	0.8079	(0.7913, 0.8144)	0.8011	(0.7857, 0.8061)	0.8008	(0.7858, 0.8055)	0.8008	(0.7858, 0.8055)
Code15	Ribeiro	MTLR	none	5	0.8162	(0.8143, 0.8264)	0.8075	(0.8027, 0.8165)	0.8008	(0.7955, 0.8081)	0.8002	(0.7953, 0.8076)	0.8002	(0.7953, 0.8076)
Code15	Ribeiro	DeepHit	none	5	0.8157	(0.7823, 0.8193)	0.8059	(0.7757, 0.8080)	0.7971	(0.7678, 0.8006)	0.7969	(0.7680, 0.8002)	0.7969	(0.7680, 0.8002)
Code15	InceptionTime	MTLR	none	5	0.8049	(0.8045, 0.8067)	0.7946	(0.7942, 0.7968)	0.7902	(0.7901, 0.7912)	0.7901	(0.7900, 0.7910)	0.7901	(0.7900, 0.7910)
Code15	InceptionTime	DeepSurv	none	5	0.8038	(0.8024, 0.8040)	0.7944	(0.7919, 0.7944)	0.7887	(0.7886, 0.7887)	0.7883	(0.7883, 0.7887)	0.7883	(0.7883, 0.7887)
Code15	InceptionTime	LH	none	5	0.7985	(0.7878, 0.8015)	0.7905	(0.7840, 0.7968)	0.7877	(0.7818, 0.7933)	0.7876	(0.7819, 0.7932)	0.7876	(0.7819, 0.7932)
Code15	Ribeiro	Cla-10	none	5	0.7961	(0.7934, 0.8035)	0.7924	(0.7891, 0.7961)	0.7872	(0.7839, 0.7889)	0.7869	(0.7838, 0.7887)	0.7869	(0.7838, 0.7887)
Code15	InceptionTime	DeepHit	none	5	0.7953	(0.7953, 0.7972)	0.7889	(0.7883, 0.7904)	0.7862	(0.7848, 0.7863)	0.786	(0.7847, 0.7861)	0.786	(0.7847, 0.7861)
Code15	Ribeiro	Cla-5	none	5	0.8029	(0.7964, 0.8035)	0.7949	(0.7881, 0.7977)	0.7858	(0.7826, 0.7899)	0.7856	(0.7825, 0.7896)	0.7856	(0.7825, 0.7896)
Code15	InceptionTime	Cla-10	none	5	0.7857	(0.7847, 0.7958)	0.7813	(0.7796, 0.7888)	0.7795	(0.7791, 0.7852)	0.7794	(0.7790, 0.7851)	0.7794	(0.7790, 0.7851)
Code15	InceptionTime	Cla-5	none	5	0.7868	(0.7835, 0.7938)	0.7812	(0.7767, 0.7860)	0.7782	(0.7745, 0.7816)	0.778	(0.7742, 0.7814)	0.778	(0.7742, 0.7814)
Code15	Ribeiro	Cla-2	none	5	0.7906	(0.7852, 0.7906)	0.7776	(0.7753, 0.7840)	0.7707	(0.7684, 0.7762)	0.7707	(0.7684, 0.7760)	0.7707	(0.7684, 0.7760)
Code15	Ribeiro	Cla-1	none	5	0.7871	(0.7826, 0.7891)	0.7739	(0.7728, 0.7753)	0.767	(0.7604, 0.7677)	0.767	(0.7602, 0.7676)	0.767	(0.7602, 0.7676)
Code15	InceptionTime	Cla-2	none	5	0.7808	(0.7761, 0.7844)	0.7716	(0.7647, 0.7780)	0.7666	(0.7582, 0.7735)	0.7666	(0.7581, 0.7734)	0.7666	(0.7581, 0.7734)
Code15	InceptionTime	Cla-1	none	5	0.753	(0.7516, 0.7600)	0.7454	(0.7428, 0.7532)	0.7422	(0.7408, 0.7485)	0.7426	(0.7408, 0.7487)	0.7426	(0.7408, 0.7487)
MIMICV	Ribeiro	LH	age, sex	5	0.7975	(0.7920, 0.7987)	0.7882	(0.7831, 0.7891)	0.7811	(0.7764, 0.7817)	0.7797	(0.7751, 0.7803)	0.7797	(0.7751, 0.7803)
MIMICV	InceptionTime	DeepHit	age, sex	5	0.7965	(0.7959, 0.7978)	0.7876	(0.7867, 0.7893)	0.7805	(0.7801, 0.7828)	0.7793	(0.7789, 0.7816)	0.7793	(0.7789, 0.7816)
MIMICV	Ribeiro	DeepHit	age, sex	5	0.7936	(0.7928, 0.7937)	0.7848	(0.7839, 0.7850)	0.7782	(0.7775, 0.7783)	0.7769	(0.7762, 0.7770)	0.7769	(0.7762, 0.7770)
MIMICV	Ribeiro	Cla-1	age, sex	5	0.7968	(0.7965, 0.7973)	0.7868	(0.7866, 0.7874)	0.7781	(0.7776, 0.7784)	0.7762	(0.7755, 0.7764)	0.7762	(0.7755, 0.7763)
MIMICV	InceptionTime	Cla-1	age, sex	5	0.7973	(0.7960, 0.7975)	0.7872	(0.7852, 0.7876)	0.7777	(0.7747, 0.7780)	0.7757	(0.7725, 0.7759)	0.7757	(0.7725, 0.7759)
MIMICV	Ribeiro	MTLR	age, sex	5	0.7933	(0.7849, 0.7934)	0.7844	(0.7763, 0.7844)	0.7768	(0.7703, 0.7774)	0.7754	(0.7691, 0.7760)	0.7754	(0.7691, 0.7760)
MIMICV	InceptionTime	MTLR	age, sex	5	0.7916	(0.7899, 0.7929)	0.7829	(0.7811, 0.7845)	0.7762	(0.7741, 0.7771)	0.775	(0.7728, 0.7757)	0.775	(0.7728, 0.7757)
MIMICV	Ribeiro	Cla-2	age, sex	5	0.7951	(0.7886, 0.7961)	0.7854	(0.7789, 0.7867)	0.7769	(0.7708, 0.7785)	0.775	(0.7690, 0.7767)	0.775	(0.7690, 0.7766)
MIMICV	InceptionTime	LH	age, sex	5	0.7931	(0.7919, 0.7957)	0.7837	(0.7834, 0.7867)	0.776	(0.7754, 0.7794)	0.7747	(0.7742, 0.7781)	0.7747	(0.7741, 0.7781)
MIMICV	InceptionTime	Cla-2	age, sex	5	0.7952	(0.7947, 0.7953)	0.7854	(0.7850, 0.7855)	0.7765	(0.7763, 0.7768)	0.7746	(0.7746, 0.7750)	0.7746	(0.7745, 0.7749)
MIMICV	Ribeiro	DeepSurv	age, sex	5	0.7866	(0.7846, 0.7871)	0.7782	(0.7768, 0.7788)	0.7717	(0.7704, 0.7723)	0.7703	(0.7690, 0.7709)	0.7703	(0.7690, 0.7709)
MIMICV	InceptionTime	DeepSurv	age, sex	5	0.7843	(0.7832, 0.7848)	0.7771	(0.7753, 0.7775)	0.7713	(0.7691, 0.7715)	0.77	(0.7678, 0.7703)	0.7699	(0.7678, 0.7702)
MIMICV	Ribeiro	Cla-5	age, sex	5	0.7872	(0.7835, 0.7886)	0.7783	(0.7748, 0.7795)	0.7712	(0.7678, 0.7724)	0.7697	(0.7664, 0.7709)	0.7697	(0.7664, 0.7709)
MIMICV	InceptionTime	Cla-5	age, sex	5	0.7832	(0.7780, 0.7871)	0.7749	(0.7701, 0.7782)	0.7688	(0.7643, 0.7714)	0.7674	(0.7630, 0.7699)	0.7674	(0.7630, 0.7699)
MIMICV	Ribeiro	Cla-10	age, sex	5	0.7787	(0.7714, 0.7819)	0.767	(0.7631, 0.7734)	0.7636	(0.7569, 0.7669)	0.7625	(0.7558, 0.7656)	0.7625	(0.7558, 0.7656)
MIMICV	InceptionTime	Cla-10	age, sex	5	0.7741	(0.7725, 0.7759)	0.7664	(0.7644, 0.7685)	0.7607	(0.7594, 0.7632)	0.7597	(0.7583, 0.7620)	0.7597	(0.7583, 0.7620)
MIMICV	FeedForward	Cla-2	age, sex	3	0.6562	(0.6562, 0.6563)	0.6552	(0.6552, 0.6553)	0.6574	(0.6573, 0.6574)	0.6578	(0.6577, 0.6578)	0.6578	(0.6577, 0.6578)
MIMICV	Ribeiro	Cla-1	age, sex, auto-ECG	3	0.7977	(0.7941, 0.7991)	0.7876	(0.7843, 0.7890)	0.7787	(0.7753, 0.7797)	0.7767	(0.7733, 0.7776)	0.7767	(0.7733, 0.7776)
MIMICV	Ribeiro	DeepHit	age, sex, auto-ECG	3	0.7928	(0.7912, 0.7937)	0.7838	(0.7824, 0.7850)	0.7768	(0.7759, 0.7781)	0.7754	(0.7745, 0.7767)	0.7754	(0.7745, 0.7767)
MIMICV	Ribeiro	LH	age, sex, auto-ECG	3	0.7923	(0.7901, 0.7942)	0.7835	(0.7810, 0.7852)	0.7763	(0.7738, 0.7779)	0.7749	(0.7725, 0.7765)	0.7749	(0.7725, 0.7765)
MIMICV	InceptionTime	DeepHit	age, sex, auto-ECG	3	0.7903	(0.7864, 0.7909)	0.7818	(0.7771, 0.7824)	0.7756	(0.7696, 0.7761)	0.7744	(0.7683, 0.7749)	0.7744	(0.7683, 0.7749)
MIMICV	InceptionTime	LH	age, sex, auto-ECG	3	0.7909	(0.7898, 0.7921)	0.7822	(0.7812, 0.7831)	0.7752	(0.7742, 0.7757)	0.7738	(0.7728, 0.7743)	0.7738	(0.7728, 0.7742)
MIMICV	InceptionTime	Cla-2	age, sex, auto-ECG	3	0.7944	(0.7923, 0.7944)	0.7844	(0.7824, 0.7845)	0.7755	(0.7739, 0.7756)	0.7735	(0.7721, 0.7736)	0.7735	(0.7721, 0.7736)
MIMICV	Ribeiro	DeepSurv	age, sex, auto-ECG	3	0.7875	(0.7868, 0.7888)	0.7798	(0.7791, 0.7808)	0.7733	(0.7727, 0.7740)	0.772	(0.7713, 0.7725)	0.772	(0.7713, 0.7725)
MIMICV	InceptionTime	Cla-1	age, sex, auto-ECG	3	0.7938	(0.7924, 0.7952)	0.7833	(0.7824, 0.7847)	0.7735	(0.7730, 0.7749)	0.7713	(0.7709, 0.7727)	0.7713	(0.7709, 0.7727)
MIMICV	Ribeiro	Cla-2	age, sex, auto-ECG	3										

Supplement Table 5

Concordance (censored to year y), bootstrapped 20x with 1 ECG per patient														
Data	Architecture	Model	Covariates	N	1-Yr	(25-75th%)	2-Yr	(25-75th%)	5-Yr	(25-75th%)	10-Yr	(25-75th%)	All-Time	(25-75th%)
Code15	Ribeiro	DeepSurv	age, sex	5	0.8333	(0.8327, 0.8335)	0.8297	(0.8289, 0.8306)	0.8278	(0.8272, 0.8283)	0.8276	(0.8270, 0.8280)	0.8276	(0.8270, 0.8280)
Code15	Ribeiro	LH	age, sex	5	0.8335	(0.8256, 0.8347)	0.8274	(0.8205, 0.8281)	0.825	(0.8213, 0.8260)	0.8248	(0.8211, 0.8256)	0.8248	(0.8211, 0.8256)
Code15	Ribeiro	MTLR	age, sex	5	0.8266	(0.8240, 0.8289)	0.8223	(0.8218, 0.8258)	0.8229	(0.8213, 0.8247)	0.8227	(0.8212, 0.8244)	0.8227	(0.8212, 0.8244)
Code15	Ribeiro	DeepHit	age, sex	5	0.8237	(0.8236, 0.8258)	0.8206	(0.8195, 0.8222)	0.8207	(0.8206, 0.8207)	0.8206	(0.8204, 0.8206)	0.8206	(0.8204, 0.8206)
Code15	InceptionTime	MTLR	age, sex	5	0.8233	(0.8214, 0.8262)	0.8193	(0.8186, 0.8220)	0.8201	(0.8196, 0.8228)	0.8201	(0.8195, 0.8225)	0.8201	(0.8195, 0.8225)
Code15	InceptionTime	DeepHit	age, sex	5	0.8231	(0.8229, 0.8233)	0.8203	(0.8192, 0.8208)	0.8198	(0.8183, 0.8217)	0.8197	(0.8183, 0.8216)	0.8197	(0.8183, 0.8216)
Code15	InceptionTime	DeepSurv	age, sex	5	0.8181	(0.8162, 0.8191)	0.8165	(0.8162, 0.8188)	0.8181	(0.8170, 0.8182)	0.8181	(0.8172, 0.8182)	0.8181	(0.8172, 0.8182)
Code15	InceptionTime	LH	age, sex	5	0.82	(0.8151, 0.8250)	0.8183	(0.8114, 0.8188)	0.8176	(0.8134, 0.8198)	0.8176	(0.8133, 0.8196)	0.8176	(0.8133, 0.8196)
Code15	Ribeiro	Cla-5	age, sex	5	0.8212	(0.8183, 0.8261)	0.8163	(0.8138, 0.8224)	0.8166	(0.8126, 0.8209)	0.8166	(0.8128, 0.8207)	0.8166	(0.8128, 0.8207)
Code15	InceptionTime	Cla-10	age, sex	5	0.8167	(0.8131, 0.8195)	0.8151	(0.8117, 0.8169)	0.8161	(0.8134, 0.8183)	0.8161	(0.8135, 0.8182)	0.8161	(0.8135, 0.8182)
Code15	Ribeiro	Cla-10	age, sex	5	0.8185	(0.8131, 0.8232)	0.8174	(0.8094, 0.8176)	0.8156	(0.8092, 0.8181)	0.8154	(0.8093, 0.8181)	0.8154	(0.8093, 0.8181)
Code15	InceptionTime	Cla-5	age, sex	5	0.8177	(0.8176, 0.8180)	0.8148	(0.8140, 0.8153)	0.8152	(0.8150, 0.8156)	0.8151	(0.8150, 0.8155)	0.8151	(0.8150, 0.8155)
Code15	Ribeiro	Cla-1	age, sex	5	0.8262	(0.8182, 0.8314)	0.8151	(0.8083, 0.8184)	0.8129	(0.8073, 0.8135)	0.8125	(0.8072, 0.8129)	0.8125	(0.8072, 0.8129)
Code15	InceptionTime	Cla-2	age, sex	5	0.8139	(0.8136, 0.8145)	0.8109	(0.8104, 0.8120)	0.8118	(0.8115, 0.8122)	0.8121	(0.8115, 0.8122)	0.8121	(0.8115, 0.8122)
Code15	Ribeiro	Cla-2	age, sex	5	0.819	(0.8150, 0.8265)	0.8098	(0.8091, 0.8182)	0.8073	(0.8065, 0.8161)	0.807	(0.8064, 0.8159)	0.807	(0.8064, 0.8159)
Code15	InceptionTime	Cla-1	age, sex	5	0.8118	(0.8081, 0.8150)	0.808	(0.8057, 0.8087)	0.8067	(0.8060, 0.8086)	0.8067	(0.8058, 0.8086)	0.8067	(0.8058, 0.8086)
Code15	FeedForward	Cla-2	age, sex	3	0.7783	(0.7780, 0.7785)	0.7843	(0.7839, 0.7845)	0.7907	(0.7902, 0.7908)	0.7908	(0.7904, 0.7910)	0.7908	(0.7904, 0.7910)
Code15	Ribeiro	DeepSurv	none	5	0.8181	(0.8141, 0.8213)	0.8122	(0.8048, 0.8137)	0.8055	(0.7986, 0.8058)	0.8051	(0.7982, 0.8051)	0.8051	(0.7982, 0.8051)
Code15	Ribeiro	LH	none	5	0.8181	(0.8007, 0.8271)	0.8079	(0.7913, 0.8144)	0.8011	(0.7857, 0.8061)	0.8008	(0.7858, 0.8055)	0.8008	(0.7858, 0.8055)
Code15	Ribeiro	MTLR	none	5	0.8162	(0.8143, 0.8264)	0.8075	(0.8027, 0.8165)	0.8008	(0.7955, 0.8081)	0.8002	(0.7953, 0.8078)	0.8002	(0.7953, 0.8078)
Code15	Ribeiro	DeepHit	none	5	0.8157	(0.7823, 0.8193)	0.8059	(0.7757, 0.8080)	0.7971	(0.7678, 0.8006)	0.7969	(0.7680, 0.8002)	0.7969	(0.7680, 0.8002)
Code15	InceptionTime	MTLR	none	5	0.8049	(0.8045, 0.8067)	0.7946	(0.7942, 0.7968)	0.7902	(0.7901, 0.7912)	0.7901	(0.7900, 0.7910)	0.7901	(0.7900, 0.7910)
Code15	InceptionTime	DeepSurv	none	5	0.8038	(0.8024, 0.8040)	0.7944	(0.7919, 0.7944)	0.7887	(0.7886, 0.7887)	0.7883	(0.7883, 0.7887)	0.7883	(0.7883, 0.7887)
Code15	InceptionTime	LH	none	5	0.7985	(0.7878, 0.8015)	0.7905	(0.7840, 0.7968)	0.7877	(0.7818, 0.7933)	0.7876	(0.7819, 0.7932)	0.7876	(0.7819, 0.7932)
Code15	Ribeiro	Cla-10	none	5	0.7961	(0.7934, 0.8035)	0.7924	(0.7891, 0.7961)	0.7872	(0.7839, 0.7889)	0.7869	(0.7838, 0.7887)	0.7869	(0.7838, 0.7887)
Code15	InceptionTime	DeepHit	none	5	0.7953	(0.7953, 0.7972)	0.7889	(0.7883, 0.7904)	0.7862	(0.7848, 0.7863)	0.786	(0.7847, 0.7861)	0.786	(0.7847, 0.7861)
Code15	Ribeiro	Cla-5	none	5	0.8029	(0.7964, 0.8035)	0.7949	(0.7881, 0.7977)	0.7858	(0.7826, 0.7899)	0.7856	(0.7825, 0.7896)	0.7856	(0.7825, 0.7896)
Code15	InceptionTime	Cla-10	none	5	0.7857	(0.7847, 0.7958)	0.7813	(0.7796, 0.7888)	0.7795	(0.7791, 0.7852)	0.7794	(0.7790, 0.7851)	0.7794	(0.7790, 0.7851)
Code15	InceptionTime	Cla-5	none	5	0.7868	(0.7835, 0.7938)	0.7812	(0.7767, 0.7860)	0.7782	(0.7745, 0.7816)	0.778	(0.7742, 0.7814)	0.778	(0.7742, 0.7814)
Code15	Ribeiro	Cla-2	none	5	0.7906	(0.7852, 0.7906)	0.7776	(0.7753, 0.7840)	0.7707	(0.7684, 0.7762)	0.7707	(0.7684, 0.7760)	0.7707	(0.7684, 0.7760)
Code15	Ribeiro	Cla-1	none	5	0.7871	(0.7826, 0.7891)	0.7739	(0.7728, 0.7753)	0.767	(0.7604, 0.7677)	0.767	(0.7602, 0.7676)	0.767	(0.7602, 0.7676)
Code15	InceptionTime	Cla-2	none	5	0.7808	(0.7761, 0.7844)	0.7716	(0.7647, 0.7780)	0.7666	(0.7582, 0.7735)	0.7666	(0.7581, 0.7734)	0.7666	(0.7581, 0.7734)
Code15	InceptionTime	Cla-1	none	5	0.753	(0.7516, 0.7600)	0.7454	(0.7428, 0.7532)	0.7422	(0.7408, 0.7485)	0.7426	(0.7408, 0.7487)	0.7426	(0.7408, 0.7487)
MIMICIV	Ribeiro	Cla-1	age, sex	5	0.8381	(0.8370, 0.8399)	0.8342	(0.8330, 0.8358)	0.8314	(0.8302, 0.8329)	0.8308	(0.8296, 0.8323)	0.8308	(0.8296, 0.8323)
MIMICIV	Ribeiro	Cla-2	age, sex	5	0.8368	(0.8316, 0.8389)	0.8329	(0.8276, 0.8349)	0.83	(0.8251, 0.8320)	0.8296	(0.8247, 0.8314)	0.8295	(0.8246, 0.8314)
MIMICIV	InceptionTime	Cla-2	age, sex	5	0.8359	(0.8348, 0.8376)	0.832	(0.8308, 0.8336)	0.8292	(0.8279, 0.8309)	0.8288	(0.8274, 0.8304)	0.8287	(0.8274, 0.8304)
MIMICIV	InceptionTime	Cla-1	age, sex	5	0.8349	(0.8336, 0.8367)	0.8309	(0.8296, 0.8330)	0.8278	(0.8265, 0.8299)	0.8272	(0.8259, 0.8293)	0.8272	(0.8259, 0.8293)
MIMICIV	Ribeiro	Cla-5	age, sex	5	0.8319	(0.8278, 0.8341)	0.8282	(0.8240, 0.8300)	0.8257	(0.8215, 0.8276)	0.8253	(0.8210, 0.8272)	0.8253	(0.8209, 0.8272)
MIMICIV	InceptionTime	Cla-5	age, sex	5	0.83	(0.8266, 0.8318)	0.8266	(0.8230, 0.8281)	0.824	(0.8210, 0.8258)	0.8236	(0.8206, 0.8255)	0.8236	(0.8206, 0.8255)
MIMICIV	Ribeiro	Cla-10	age, sex	5	0.8266	(0.8196, 0.8290)	0.8227	(0.8161, 0.8254)	0.8202	(0.8139, 0.8231)	0.8199	(0.8134, 0.8226)	0.8199	(0.8134, 0.8226)
MIMICIV	InceptionTime	Cla-10	age, sex	5	0.8248	(0.8229, 0.8259)	0.8212	(0.8193, 0.8226)	0.8192	(0.8171, 0.8206)	0.8188	(0.8169, 0.8202)	0.8188	(0.8169, 0.8202)
MIMICIV	InceptionTime	DeepHit	age, sex	5	0.8242	(0.8227, 0.8256)	0.8208	(0.8196, 0.8225)	0.819	(0.8177, 0.8205)	0.8187	(0.8174, 0.8203)	0.8187	(0.8174, 0.8203)
MIMICIV	Ribeiro	LH	age, sex	5	0.8231	(0.8205, 0.8258)	0.8197	(0.8171, 0.8226)	0.8175	(0.8148, 0.8205)	0.8172	(0.8144, 0.8202)	0.8172	(0.8144, 0.8202)
MIMICIV	Ribeiro	DeepHit	age, sex	5	0.8213	(0.8198, 0.8226)	0.8179	(0.8167, 0.8193)	0.816	(0.8148, 0.8172)	0.8157	(0.8145, 0.8169)	0.8157	(0.8145, 0.8169)
MIMICIV	InceptionTime	LH	age, sex	5	0.8204	(0.8177, 0.8228)	0.8171	(0.8143, 0.8192)	0.8151	(0.8121, 0.8171)	0.8148	(0.8118, 0.8168)	0.8148	(0.8118, 0.8168)
MIMICIV	Ribeiro	MTLR	age, sex	5	0.8198	(0.8160, 0.8217)	0.8162	(0.8128, 0.8184)	0.8141	(0.8109, 0.8162)	0.8138	(0.8106, 0.8159)	0.8138	(0.8106, 0.8159)
MIMICIV	InceptionTime	MTLR	age, sex	5	0.8187	(0.8166, 0.8218)	0.8153	(0.8136, 0.8185)	0.8134	(0.8117, 0.8164)	0.8131	(0.8113, 0.8162)	0.8131	(0.8113, 0.8162)
MIMICIV	InceptionTime	DeepSurv	age, sex	5	0.8183	(0.8171, 0.8199)	0.8153	(0.8142, 0.8167)	0.8134	(0.8121, 0.8148)	0.8131	(0.8118, 0.8145)	0.8131	(0.8118, 0.8145)
MIMICIV	Ribeiro	DeepSurv	age, sex	5	0.8173	(0.8132, 0.8198)	0.8138	(0.8104, 0.8165)	0.8115	(0.8086, 0.8143)	0.8112	(0.8081, 0.8140)	0.8112	(0.8081, 0.8140)
MIMICIV	FeedForward	Cla-10	age, sex	3	0.7291	(0.7279, 0.7302)	0.7281	(0.7269, 0.7288)	0.728	(0.7269, 0.7286)	0.7281	(0.7270, 0.7286)	0.7281	(0.7270, 0.7286)
MIMICIV	FeedForward	Cla-2	age, sex	3	0.729	(0.7278, 0.7302)	0.728	(0.7268, 0.7288)	0.7279	(0.7270, 0.7286)	0.728	(0.7271, 0.7286)	0.728	(0.7271, 0.7286)
MIMICIV	Ribeiro	Cla-1	age, sex, auto-ECG	3	0.8377	(0.8343, 0.8392)	0.8339	(0.8301, 0.8349)	0.8308	(0.8270, 0.8319)	0.8302	(0.8265, 0.8314)	0.8302	(0.8265, 0.8314)
MIMICIV	InceptionTime	Cla-1	age, sex, auto-ECG	3	0.8345	(0.8328, 0.8355)	0.8305	(0.8288, 0.8313)	0.8274	(0.8257, 0.8283)	0.8269	(0.8251, 0.8277)	0.8268	(0.8250, 0.8277)
MIMICIV	Ribeiro	Cla-2	age, sex, auto-ECG	3	0.8336	(0.8214, 0.8379)	0.8295	(0.8178, 0.8341)	0.8265	(0.8154, 0.8313)	0.826	(0.8149, 0.8308)	0.826	(0.8149, 0.8308)
MIMICIV	InceptionTime	Cla-2	age, sex, auto-ECG	3	0.8326	(0.8318, 0.8338)	0.8286	(0.8277, 0.8296)	0.8259	(0.8249, 0.8270)	0.8254	(0.8243, 0.8264)	0.8254	(0.8243, 0.8264)
MIMICIV	Ribeiro	Cla-5	age, sex, auto-ECG	3	0.8324	(0.8286, 0.8335)	0.8283	(0.8250, 0.8294)	0.8257	(0.8225, 0.8269)	0.8254	(0.8221, 0.8265)	0.8254	(0.8221, 0.8265)
MIMICIV	InceptionTime	Cla-5	age, sex, auto-ECG	3	0.8307	(0.8275, 0.8327)	0.8269	(0.8238, 0.8290)	0.8247	(0.8215, 0.8265)	0.8243	(0.8211, 0.8261)	0.8243	(0.8211, 0.8261)
MIMICIV	Ribeiro	Cla-10	age, sex, auto-ECG	3	0.8264	(0.8257, 0.8275)	0.8228	(0.8220, 0.8236)	0.8204	(0.8196, 0.8213)	0.82	(0.8193, 0.8210)	0.82	(0.8193, 0.8210)
MIMICIV	InceptionTime	Cla-10	age, sex											

Supplement Table 6

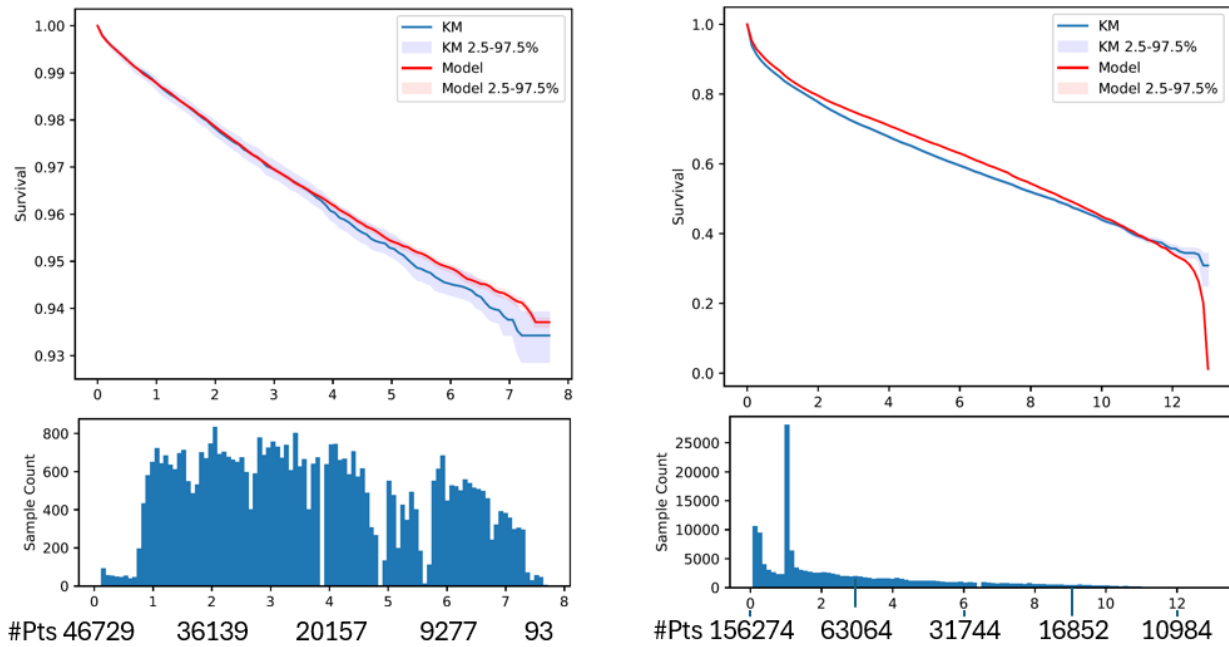
Data	Architecture	Model	Covariates	N	AUROC					AUPRC				
					1-Yr (25-75th%)	2-Yr (25-75th%)	5-Yr (25-75th%)	10-Yr (25-75th%)	1-Yr (25-75th%)	2-Yr (25-75th%)	5-Yr (25-75th%)	10-Yr (25-75th%)		
Code15	Ribeiro	DeepSurv	age, sex	5	0.84 (0.83, 0.84)	0.83 (0.83, 0.83)	0.83 (0.83, 0.84)	0.83 (0.83, 0.84)	0.83 (0.83, 0.84)	0.08 (0.07, 0.08)	0.11 (0.10, 0.11)	0.15 (0.15, 0.15)	0.16 (0.15, 0.16)	
Code15	Ribeiro	LH	age, sex	5	0.83 (0.83, 0.84)	0.83 (0.82, 0.83)	0.83 (0.83, 0.83)	0.83 (0.83, 0.83)	0.83 (0.83, 0.83)	0.07 (0.06, 0.07)	0.09 (0.09, 0.10)	0.14 (0.14, 0.14)	0.15 (0.14, 0.15)	
Code15	Ribeiro	MTLR	age, sex	5	0.83 (0.83, 0.83)	0.83 (0.82, 0.83)	0.83 (0.83, 0.83)	0.83 (0.83, 0.83)	0.83 (0.83, 0.83)	0.07 (0.07, 0.07)	0.10 (0.10, 0.10)	0.14 (0.14, 0.14)	0.15 (0.15, 0.15)	
Code15	Ribeiro	DeepHit	age, sex	5	0.83 (0.83, 0.83)	0.83 (0.82, 0.83)	0.83 (0.83, 0.83)	0.83 (0.83, 0.83)	0.17 (0.17, 0.18)	0.07 (0.06, 0.07)	0.09 (0.09, 0.10)	0.14 (0.13, 0.14)	0.02 (0.02, 0.02)	
Code15	Ribeiro	MTLR	age, sex	5	0.83 (0.82, 0.83)	0.82 (0.82, 0.83)	0.83 (0.83, 0.83)	0.83 (0.83, 0.83)	0.83 (0.83, 0.83)	0.07 (0.07, 0.07)	0.10 (0.10, 0.10)	0.15 (0.14, 0.15)	0.15 (0.15, 0.15)	
Code15	InceptionTime	DeepHit	age, sex	5	0.82 (0.82, 0.82)	0.82 (0.82, 0.82)	0.83 (0.83, 0.83)	0.18 (0.17, 0.18)	0.07 (0.06, 0.07)	0.09 (0.09, 0.10)	0.14 (0.14, 0.14)	0.02 (0.02, 0.02)		
Code15	InceptionTime	DeepSurv	age, sex	5	0.82 (0.82, 0.82)	0.82 (0.82, 0.82)	0.83 (0.82, 0.83)	0.83 (0.83, 0.83)	0.83 (0.83, 0.83)	0.07 (0.06, 0.07)	0.10 (0.09, 0.10)	0.14 (0.14, 0.14)	0.15 (0.15, 0.15)	
Code15	InceptionTime	LH	age, sex	5	0.82 (0.82, 0.83)	0.82 (0.82, 0.82)	0.83 (0.82, 0.83)	0.83 (0.82, 0.83)	0.83 (0.82, 0.83)	0.07 (0.06, 0.07)	0.09 (0.09, 0.10)	0.14 (0.14, 0.15)	0.15 (0.14, 0.15)	
Code15	Ribeiro	Cla-5	age, sex	5	0.82 (0.82, 0.83)	0.82 (0.82, 0.83)	0.82 (0.82, 0.83)	0.83 (0.82, 0.83)	0.83 (0.82, 0.83)	0.06 (0.06, 0.07)	0.09 (0.08, 0.09)	0.14 (0.13, 0.14)	0.15 (0.14, 0.15)	
Code15	InceptionTime	Cla-10	age, sex	5	0.82 (0.82, 0.82)	0.82 (0.82, 0.82)	0.83 (0.82, 0.83)	0.83 (0.82, 0.83)	0.83 (0.82, 0.83)	0.06 (0.06, 0.06)	0.09 (0.09, 0.10)	0.14 (0.14, 0.14)	0.15 (0.15, 0.15)	
Code15	Ribeiro	Cla-10	age, sex	5	0.82 (0.81, 0.83)	0.82 (0.81, 0.82)	0.82 (0.82, 0.83)	0.82 (0.82, 0.83)	0.82 (0.82, 0.83)	0.06 (0.06, 0.06)	0.09 (0.09, 0.09)	0.13 (0.13, 0.13)	0.14 (0.14, 0.14)	
Code15	InceptionTime	Cla-5	age, sex	5	0.82 (0.82, 0.82)	0.82 (0.82, 0.82)	0.82 (0.82, 0.82)	0.83 (0.82, 0.83)	0.83 (0.82, 0.83)	0.06 (0.06, 0.06)	0.09 (0.09, 0.09)	0.14 (0.14, 0.14)	0.15 (0.14, 0.15)	
Code15	Ribeiro	Cla-1	age, sex	5	0.83 (0.82, 0.83)	0.82 (0.81, 0.82)	0.82 (0.81, 0.82)	0.82 (0.81, 0.82)	0.82 (0.81, 0.82)	0.07 (0.07, 0.07)	0.09 (0.09, 0.10)	0.14 (0.14, 0.14)	0.14 (0.14, 0.14)	
Code15	InceptionTime	Cla-2	age, sex	5	0.82 (0.82, 0.82)	0.81 (0.81, 0.82)	0.82 (0.82, 0.82)	0.82 (0.82, 0.82)	0.82 (0.82, 0.82)	0.06 (0.06, 0.06)	0.09 (0.09, 0.09)	0.14 (0.13, 0.14)	0.14 (0.14, 0.15)	
Code15	Ribeiro	Cla-2	age, sex	5	0.82 (0.82, 0.83)	0.81 (0.81, 0.82)	0.81 (0.81, 0.82)	0.81 (0.81, 0.82)	0.81 (0.81, 0.82)	0.06 (0.06, 0.06)	0.08 (0.08, 0.09)	0.13 (0.13, 0.13)	0.13 (0.13, 0.13)	
Code15	InceptionTime	Cla-1	age, sex	5	0.81 (0.81, 0.82)	0.81 (0.81, 0.81)	0.81 (0.81, 0.82)	0.82 (0.81, 0.82)	0.82 (0.81, 0.82)	0.06 (0.06, 0.06)	0.09 (0.09, 0.09)	0.13 (0.13, 0.14)	0.14 (0.14, 0.14)	
Code15	FeedForward	Cla-2	age, sex	3	0.78 (0.78, 0.78)	0.79 (0.79, 0.79)	0.80 (0.80, 0.80)	0.81 (0.81, 0.81)	0.81 (0.81, 0.81)	0.04 (0.04, 0.04)	0.07 (0.07, 0.07)	0.11 (0.11, 0.11)	0.12 (0.12, 0.12)	
Code15	Ribeiro	DeepSurv	none	5	0.82 (0.82, 0.82)	0.82 (0.81, 0.82)	0.81 (0.80, 0.81)	0.81 (0.80, 0.81)	0.81 (0.80, 0.81)	0.07 (0.07, 0.07)	0.10 (0.10, 0.10)	0.14 (0.14, 0.14)	0.14 (0.14, 0.15)	
Code15	Ribeiro	LH	none	5	0.82 (0.80, 0.83)	0.81 (0.79, 0.81)	0.80 (0.79, 0.81)	0.80 (0.79, 0.80)	0.80 (0.79, 0.80)	0.07 (0.06, 0.08)	0.10 (0.09, 0.10)	0.14 (0.13, 0.14)	0.14 (0.13, 0.14)	
Code15	Ribeiro	MTLR	none	5	0.82 (0.82, 0.83)	0.81 (0.80, 0.82)	0.80 (0.80, 0.81)	0.80 (0.80, 0.80)	0.80 (0.80, 0.80)	0.07 (0.07, 0.08)	0.10 (0.10, 0.10)	0.14 (0.13, 0.14)	0.14 (0.14, 0.14)	
Code15	Ribeiro	DeepHit	none	5	0.82 (0.78, 0.82)	0.81 (0.78, 0.81)	0.80 (0.77, 0.80)	0.20 (0.20, 0.23)	0.07 (0.05, 0.07)	0.09 (0.07, 0.10)	0.13 (0.10, 0.13)	0.02 (0.02, 0.02)		
Code15	InceptionTime	MTLR	none	5	0.81 (0.81, 0.81)	0.80 (0.80, 0.80)	0.80 (0.80, 0.80)	0.79 (0.79, 0.80)	0.79 (0.79, 0.80)	0.06 (0.06, 0.07)	0.09 (0.09, 0.09)	0.13 (0.13, 0.13)	0.13 (0.13, 0.13)	
Code15	InceptionTime	DeepSurv	none	5	0.81 (0.80, 0.81)	0.80 (0.79, 0.80)	0.79 (0.79, 0.79)	0.80 (0.79, 0.80)	0.80 (0.79, 0.80)	0.06 (0.06, 0.06)	0.08 (0.08, 0.09)	0.12 (0.12, 0.13)	0.13 (0.13, 0.14)	
Code15	InceptionTime	LH	none	5	0.80 (0.79, 0.80)	0.79 (0.79, 0.80)	0.79 (0.79, 0.80)	0.79 (0.79, 0.80)	0.79 (0.79, 0.80)	0.06 (0.06, 0.06)	0.09 (0.08, 0.09)	0.12 (0.12, 0.13)	0.13 (0.13, 0.13)	
Code15	Ribeiro	Cla-10	none	5	0.80 (0.80, 0.81)	0.80 (0.79, 0.80)	0.79 (0.79, 0.79)	0.79 (0.79, 0.80)	0.79 (0.79, 0.80)	0.06 (0.06, 0.06)	0.08 (0.08, 0.09)	0.12 (0.12, 0.13)	0.13 (0.13, 0.13)	
Code15	InceptionTime	DeepHit	none	5	0.80 (0.80, 0.80)	0.79 (0.79, 0.79)	0.79 (0.79, 0.79)	0.21 (0.21, 0.21)	0.06 (0.06, 0.06)	0.08 (0.08, 0.08)	0.12 (0.12, 0.12)	0.02 (0.02, 0.02)		
Code15	Ribeiro	Cla-5	none	5	0.80 (0.80, 0.81)	0.80 (0.79, 0.80)	0.79 (0.79, 0.79)	0.79 (0.79, 0.80)	0.79 (0.79, 0.80)	0.06 (0.06, 0.06)	0.09 (0.08, 0.09)	0.12 (0.12, 0.12)	0.13 (0.13, 0.13)	
Code15	InceptionTime	Cla-10	none	5	0.79 (0.79, 0.80)	0.78 (0.78, 0.79)	0.79 (0.79, 0.79)	0.79 (0.79, 0.79)	0.79 (0.79, 0.79)	0.06 (0.06, 0.06)	0.08 (0.08, 0.08)	0.12 (0.12, 0.12)	0.13 (0.13, 0.13)	
Code15	InceptionTime	Cla-5	none	5	0.79 (0.78, 0.80)	0.78 (0.78, 0.79)	0.79 (0.78, 0.79)	0.79 (0.78, 0.79)	0.79 (0.78, 0.79)	0.05 (0.05, 0.06)	0.08 (0.08, 0.08)	0.12 (0.12, 0.12)	0.13 (0.13, 0.13)	
Code15	Ribeiro	Cla-2	none	5	0.79 (0.79, 0.79)	0.78 (0.78, 0.79)	0.78 (0.77, 0.78)	0.78 (0.77, 0.78)	0.78 (0.77, 0.78)	0.06 (0.06, 0.06)	0.08 (0.08, 0.08)	0.12 (0.12, 0.12)	0.12 (0.12, 0.13)	
Code15	Ribeiro	Cla-1	none	5	0.79 (0.78, 0.79)	0.77 (0.77, 0.78)	0.77 (0.76, 0.77)	0.77 (0.76, 0.77)	0.77 (0.76, 0.77)	0.06 (0.06, 0.06)	0.08 (0.08, 0.08)	0.11 (0.11, 0.12)	0.12 (0.11, 0.13)	
Code15	InceptionTime	Cla-2	none	5	0.78 (0.78, 0.79)	0.77 (0.77, 0.78)	0.77 (0.76, 0.78)	0.77 (0.76, 0.78)	0.77 (0.76, 0.78)	0.06 (0.06, 0.06)	0.08 (0.08, 0.08)	0.12 (0.12, 0.12)	0.13 (0.12, 0.13)	
Code15	InceptionTime	Cla-1	none	5	0.75 (0.75, 0.76)	0.75 (0.74, 0.76)	0.75 (0.74, 0.75)	0.75 (0.75, 0.75)	0.75 (0.75, 0.75)	0.05 (0.05, 0.06)	0.08 (0.07, 0.08)	0.11 (0.11, 0.11)	0.12 (0.12, 0.12)	
MIMICIV	Ribeiro	LH	age, sex	5	0.82 (0.81, 0.82)	0.81 (0.80, 0.81)	0.79 (0.79, 0.79)	0.78 (0.77, 0.78)	0.78 (0.77, 0.78)	0.45 (0.44, 0.46)	0.49 (0.48, 0.49)	0.55 (0.54, 0.55)	0.55 (0.55, 0.55)	
MIMICIV	InceptionTime	DeepHit	age, sex	5	0.82 (0.82, 0.82)	0.81 (0.80, 0.81)	0.78 (0.78, 0.78)	0.75 (0.75, 0.76)	0.75 (0.75, 0.76)	0.45 (0.45, 0.45)	0.49 (0.48, 0.49)	0.52 (0.52, 0.52)	0.49 (0.48, 0.50)	
MIMICIV	Ribeiro	DeepHit	age, sex	5	0.82 (0.81, 0.82)	0.80 (0.80, 0.81)	0.79 (0.78, 0.79)	0.76 (0.76, 0.76)	0.76 (0.76, 0.76)	0.44 (0.44, 0.45)	0.48 (0.48, 0.48)	0.52 (0.51, 0.52)	0.50 (0.49, 0.51)	
MIMICIV	Ribeiro	Cla-1	age, sex	5	0.82 (0.82, 0.82)	0.81 (0.81, 0.81)	0.79 (0.79, 0.79)	0.78 (0.78, 0.78)	0.78 (0.78, 0.78)	0.45 (0.45, 0.45)	0.49 (0.49, 0.49)	0.55 (0.55, 0.55)	0.56 (0.56, 0.56)	
MIMICIV	InceptionTime	Cla-1	age, sex	5	0.82 (0.81, 0.82)	0.81 (0.80, 0.81)	0.79 (0.78, 0.79)	0.77 (0.77, 0.77)	0.77 (0.77, 0.77)	0.45 (0.45, 0.45)	0.49 (0.49, 0.49)	0.54 (0.54, 0.54)	0.55 (0.55, 0.56)	
MIMICIV	Ribeiro	MTLR	age, sex	5	0.81 (0.81, 0.82)	0.80 (0.80, 0.80)	0.79 (0.79, 0.79)	0.77 (0.77, 0.77)	0.77 (0.77, 0.77)	0.44 (0.43, 0.45)	0.48 (0.47, 0.49)	0.54 (0.54, 0.54)	0.54 (0.54, 0.54)	
MIMICIV	InceptionTime	MTLR	age, sex	5	0.81 (0.81, 0.81)	0.80 (0.80, 0.80)	0.79 (0.78, 0.79)	0.77 (0.76, 0.77)	0.77 (0.76, 0.77)	0.44 (0.44, 0.44)	0.48 (0.48, 0.49)	0.54 (0.53, 0.54)	0.53 (0.53, 0.53)	
MIMICIV	Ribeiro	Cla-2	age, sex	5	0.82 (0.81, 0.82)	0.81 (0.80, 0.81)	0.79 (0.79, 0.79)	0.78 (0.77, 0.78)	0.78 (0.77, 0.78)	0.44 (0.43, 0.44)	0.48 (0.47, 0.49)	0.54 (0.54, 0.55)	0.56 (0.55, 0.56)	
MIMICIV	InceptionTime	LH	age, sex	5	0.82 (0.81, 0.82)	0.81 (0.80, 0.81)	0.79 (0.79, 0.79)	0.77 (0.77, 0.77)	0.77 (0.77, 0.77)	0.45 (0.45, 0.45)	0.49 (0.49, 0.49)	0.54 (0.53, 0.54)	0.53 (0.53, 0.54)	
MIMICIV	InceptionTime	Cla-2	age, sex	5	0.81 (0.81, 0.81)	0.80 (0.80, 0.80)	0.79 (0.79, 0.79)	0.78 (0.77, 0.78)	0.78 (0.77, 0.78)	0.44 (0.44, 0.44)	0.48 (0.48, 0.49)	0.54 (0.54, 0.54)	0.56 (0.56, 0.56)	
MIMICIV	Ribeiro	DeepSurv	age, sex	5	0.81 (0.81, 0.81)	0.80 (0.80, 0.80)	0.79 (0.79, 0.79)	0.78 (0.78, 0.78)	0.78 (0.78, 0.78)	0.44 (0.43, 0.44)	0.48 (0.48, 0.48)	0.54 (0.54, 0.54)	0.56 (0.56, 0.56)	
MIMICIV	InceptionTime	DeepSurv	age, sex	5	0.81 (0.81, 0.81)	0.80 (0.80, 0.80)	0.79 (0.79, 0.79)	0.78 (0.78, 0.78)	0.78 (0.78, 0.78)	0.43 (0.43, 0.44)	0.48 (0.48, 0.48)	0.54 (0.54, 0.55)	0.56 (0.56, 0.56)	
MIMICIV	Ribeiro	Cla-5	age, sex	5	0.81 (0.80, 0.81)	0.80 (0.80, 0.80)	0.79 (0.79, 0.79)	0.78 (0.78, 0.78)	0.78 (0.78, 0.78)	0.42 (0.42, 0.43)	0.47 (0.47, 0.48)	0.54 (0.54, 0.54)	0.56 (0.56, 0.56)	
MIMICIV	InceptionTime	Cla-5	age, sex	5	0.80 (0.80, 0.81)	0.80 (0.79, 0.80)	0.79 (0.78, 0.79)	0.78 (0.78, 0.78)	0.78 (0.78, 0.78)	0.42 (0.42, 0.42)	0.47 (0.46, 0.47)	0.54 (0.54, 0.54)	0.56 (0.56, 0.56)	
MIMICIV	Ribeiro	Cla-10	age, sex	5	0.80 (0.79, 0.80)	0.79 (0.79, 0.80)	0.79 (0.78, 0.79)	0.78 (0.78, 0.78)	0.78 (0.78, 0.78)	0.41 (0.40, 0.42)	0.46 (0.45, 0.47)	0.53 (0.53, 0.54)	0.56 (0.55, 0.56)	
MIMICIV	InceptionTime	Cla-10	age, sex	5	0.79 (0.79, 0.80)	0.79 (0.79, 0.79)	0.79 (0.79, 0.79)	0.78 (0.78, 0.78)	0.78 (0.78, 0.78)	0.41 (0.40, 0.41)	0.46 (0.46, 0.46)	0.54 (0.53, 0.54)	0.56 (0.55, 0.56)	
MIMICIV	FeedForward	Cla-2	age, sex	3	0.68 (0.68, 0.68)	0.68 (0.68, 0.68)	0.70 (0.70, 0.70)	0.70 (0.70, 0.70)	0.70 (0.70, 0.70)	0.26 (0.26, 0.26)	0.32 (0.32, 0.32)	0.42 (0.42, 0.42)	0.45 (0.45, 0.45)	
MIMICIV	Ribeiro	Cla-1	age, sex, auto-ECG	3	0.82 (0.81, 0.82)	0.81 (0.80, 0.81)	0.79 (0.79, 0.79)	0.78 (0.77, 0.78)	0.78 (0.77, 0.78)	0.45 (0.44, 0.45)	0.49 (0.49, 0.49)	0.54 (0.54, 0.55)	0.56 (0.55, 0.56)	
MIMICIV	Ribeiro	DeepHit	age, sex, auto-ECG											

Supplemental Table 7

	% of ECGs associated with mortality by year $h$				
	1-Yr	2-Yr	5-Yr	10-Yr	Max-Yr
Code-15	1.2%	2.1%	3.4%	3.6%	3.6%
MIMIC-IV	14.8%	18.4%	24.5%	27.6%	27.8%
BCH	0.9%	1.5%	3.1%	4.8%	6.9%

Supplemental Table 7. Percentage of ECGs associated with a mortality by year  $h$ .

## Supplemental Figure 1

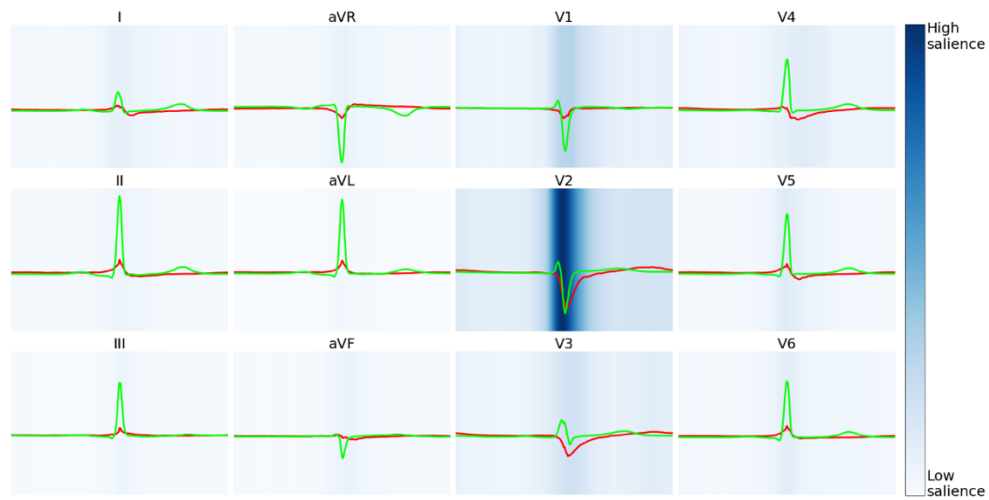


(a) Code-15

(b) MIMIC-IV

*Supplemental Figure 1.* Kaplan-Meier and population-averaged survival functions for the highest-concordance-index non-demographic Code-15 (left) and MIMIC-IV (right) models. Bottom subplots show sample count at each time point. Plots show median and 95% confidence intervals per time point (100) over 100 bootstraps. Red values indicate the number of patients under observation. Note differences in scale.

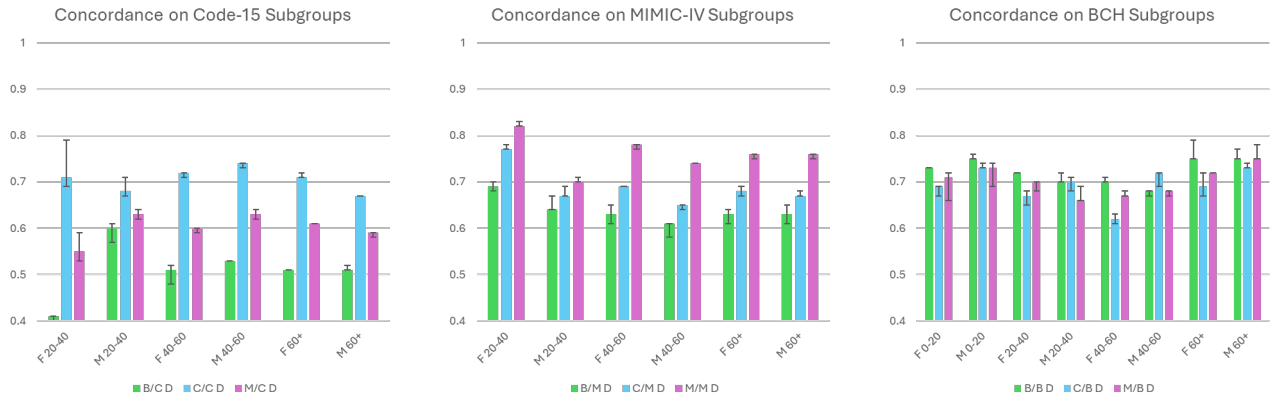
## Supplemental Figure 2



*Supplemental Figure 2.* Median heartbeats and SHAP analysis for a MIMIC Cla-5 ResNet [8]. Green: median heartbeat for 100 ECGs with lowest-risk-estimate (mean prediction probability: 0%). Red: median heartbeat for 100 ECGs with highest-risk-estimate (mean prediction probability: 69%). Blue shading: SHAP salience.

The median high-risk waveforms show lower amplitude and QRS complexes, as well as flattened/inverted lateral precordial T waves indicating several pathological findings (delayed myocardial activation, possibly myocardial strain). The QRS complex is most salient, suggesting focus mostly on myocardial activation (heartbeat dynamics). High salience of the V2 lead indicates anteroseptal activation and aligns with analyses of left ventricular (LV) dysfunction.

### Supplemental Figure 3



		Age		[0,20)		[20,40)		[40,60)		60+							
Sex		F	M	F	M	F	M	F	M	F	M						
BCH	Events, N	1552	34137	2073	40091	693	6680	915	6220	427	1815	469	1407	80	351	92	239
MIMIC-IV	Events, N	9	533	2	314	642	9470	731	7233	3293	21335	5165	24503	15974	46062	17641	46824
Code-15	Events, N	2	1125	3	918	29	8331	37	5316	96	8410	130	5206	651	9868	740	7555

*Supplemental Figure 3.* Median (IQR) model Concordance per patient subgroup. The title indicates the test set, the colors indicate the training set (Green – BCH, Blue – Code-15, Purple – MIMIC). All cases are Resnet LogisticHazard with ECG/Age/Sex. Code-15 and MIMIC-IV 0-20 not shown due to low event count. Models tend to perform better on their own test set, with one possible exception: Code-15 on BCH M40-60.